FINAL REPORT

FOR
D-1, MEA/A-2 EXPERIMENT 81FO1
CONDUCTED ON STS-61A FLIGHT, OCTOBER 1985

CONTRACT NAS 8-34758
CONTAINERLESS PROCESSING OF GLASS FORMING MELTS

(NASA-CR-179118) CONTAINERLESS PROCESSING OF GLASS FORMING MELTS: D-1, MEA/A-2 EXPERIMENT 81F01 CONDUCTED ON STS-61A FLIGHT, OCTOBER 1985 Final Report (Missouri Univ.) 63 p Avail: NTIS EC A05/MF A01 G3/27 N87-22861 Unclas 0079005

Prepared for
National Aeronautics and Space Administration
George C. Marshall Space Flight Center
Huntsville, AL 35812

Prepared by
D.E. Day and C.S. Ray
Department of Ceramic Engineering and
Graduate Center for Materials Research
University of Missouri-Rolla
Rolla, MO 65401-0249
(314) 341-4354

1 November 1986

FINAL REPORT

FOR

D-1, MEA/A-2 EXPERIMENT 81F01

CONTRACT NAS 8-34758

CONTAINERLESS PROCESSING OF GLASS FORMING MELTS

Prepared for

National Aeronautics and Space Administration

George C. Marshall Space Flight Center

Huntsville, AL 35812

Prepared by

D. E. Day and C. S. Ray

Department of Ceramic Engineering and

Graduate Center for Materials Research

University of Missouri-Rolla

Rolla, MO 65401

(314) 341-4354

Sponsored by
Microgravity Science and Applications Division
Office of Space Science and Applications
NASA Headquarters

1 November 1986

TABLE OF CONTENTS

	Page
LIST OF FIGURES	iii
LIST OF TABLES	vi
EXECUTIVE SUMMARY	1
I. INTRODUCTION	3
A. Rationale for Processing Glass in Space	3
B. Objectives of the D-1, MEA/A-2 Experiment	4
II. PREPARATION AND HANDLING OF PRECURSOR SAMPLES	11
III. PROPERTY ANALYSIS OF TERRESTRIALLY PREPARED SAMPLES	23
IV. REMOVAL AND HANDLING OF POST-FLIGHT SAMPLES	32
V. POST-FLIGHT SAMPLE ANALYSIS	33
A. Visual Examination	33
B. Weight Change	33
C. Film and Flight Data	38
D. Analysis by Scanning Electron Microscopy (SEM)	39
E. Comparison of Properties for the Glasses Melted in MEA/A-2 and on Earth	63
VI. CONCLUSIONS	68
VII. ACKNOWLEDGEMENT	71
REFERENCES	73
APPENDIX A: List of Publications Supported by the Present Contract, NAS 8-34758	75

LIST OF FIGURES

Page

Figure 1. Typical time-temperature-transformation (TTT) diagram for a glass forming material showing critical cooling rate (R_c) for glass formation 9

Figure 2. Hot pressed 35.7 CaO-39.3 Ga_2O_3-25 SiO_2, mol%, precursor sample (#2) used in D-1, MEA/A-2 15

Figure 3. Devitrified 35.7 CaO-39.3 Ga_2O_3-25 SiO_2, mol%, glass sample (#4) with colored spot used in D-1, MEA/A-2 16

Figure 4. Devitrified 44 CaO-56 Ga_2O_3, mol%, glass sample (#6) used in D-1, MEA/A-2 17

Figure 5. Hot pressed 50 PbO-50 SiO_2, mol%, sample (#7) used in D-1, MEA/A-2 18

Figure 6. TTT diagram for the 35.7 CaO-39.3 Ga_2O_3-25 SiO_2, mol%, composition for sample diameter ~3.5 mm 25

Figure 7. Dependence of the cooling rate measured on earth for glass formation upon sample diameter for the 35.7 CaO-39.3 Ga_2O_3-25 SiO_2, mol%, composition 26

Figure 8. Appearance of the interior of the hot pressed 35.7 CaO-39.3 Ga_2O_3-25 SiO_2, mol%, precursor as seen by SEM 28

Figure 9. Magnified view of a silica particle in the fracture surface of the 35.7 CaO-39.3 Ga_2O_3-25 SiO_2, mol%, hot pressed precursor 29

Figure 10. Appearance of the interior of the hot pressed 50 PbO-50 SiO_2, mol%, precursor as seen by SEM 30

Figure 11. Flight sample 2 (35.7 CaO-39.3 Ga_2O_3-25 SiO_2, mol%, hot pressed) stuck to platinum wire cage while levitated and melted in space (MEA/A-2) 35

Figure 12. Flight sample 2 (35.7 CaO-39.3 Ga_2O_3-25 SiO_2, mol%, hot pressed), MEA/A-2, with the imbedded platinum wires 36

Figure 13. The planned and observed time-temperature profile for 35.7 CaO-39.3 Ga_2O_3-25 SiO_2, mol%, hot pressed sample (#2) when processed in the single axis acoustic levitator, MEA/A-2 . . 41

Figure 14. The planned and observed time-temperature profile for the soda-lime-silica glass shell (#3) processed in the acoustic levitator, MEA/A-2 42

Figure 15. Appearance of flight sample 2 (35.7 CaO-39.3 Ga_2O_3-25 SiO_2, mol%, hot pressed) when removed from the cage wires 44

Figure 16. External surface of flight sample 2 (35.7 CaO-39.3 Ga_2O_3-25 SiO_2, mol%, hot pressed) in the vicinity of the vertical platinum wire shown imbedded in the sample in Fig. 11 45

Figure 17. SEM of the external surface of the vertical platinum wire imbedded in the flight sample 2 46

Figure 18. Crystallization found on the external surface of flight sample 2 (35.7 CaO-39.3 Ga_2O_3-25 SiO_2, mol%, hot pressed) . . 47

Figure 19. Microstructure of the external surface of flight sample 2 (35.7 CaO-39.3 Ga_2O_3-25 SiO_2, mol%, hot pressed) showing crystal concentration at different distances from the vertical platinum wire imbedded in the sample 49

Figure 20. Pieces of flight sample 2 (35.7 CaO-39.3 Ga_2O_3-25 SiO_2 mol%, hot pressed) showing the interior fracture surface examined by SEM 51

Figure 21. Composition of the external surface and the interior of flight sample 2 (35.7 CaO-39.3 Ga_2O_3-25 SiO_2, hot pressed) as determined by EDAX 52

Figure 22. General appearance in the interior of sample 2 (35.7 CaO-39.3 Ga_2O_3-25 SiO_2, mol%, hot pressed) 54

Figure 23. Summary of analysis for the external surface of sample 2 (35.7 CaO-39.3 Ga_2O_3-25 SiO_2, mol%, hot pressed) 55

Figure 24. Summary of analysis for the interior of sample 2 (35.7 CaO-39.3 Ga_2O_3-25 SiO_2, mol%, hot pressed) 56

Figure 25. The estimated TTT diagram for the 35.7 CaO-39.3 Ga_2O_3-25 SiO_2, mol%, composition for sample diameter ~6.5 mm and the cooling rate measured for sample 2 in MEA/A-2 58

Figure 26. Radiographs of the pre- and post-flight sample 3 (soda-lime-silica glass shell) 60

Figure 27. DTA thermogram for the 35.7 CaO-39.3 Ga_2O_3-25 SiO_2, mol%, glasses melted in space (MEA/A-2) and on earth 65

Figure 28. IR transmission for the 35.7 CaO-39.3 Ga_2O_3-25 SiO_2, mol%, glasses melted in space (MEA/A-2) and on earth 66

Figure 29. IR transmission for the devitrified 35.7 CaO-39.3 Ga_2O_3-25 SiO_2, mol%, glasses melted in space (MEA/A-2) and on earth 67

LIST OF TABLES

		Page
Table I.	Sample processing order, precursor description and time-line for MEA/A-2 Experiment 81F01, conducted on STS-61A, 31 October 1985	5
Table II.	Initial weight, diameter and density of precursor samples, as prepared	20
Table III.	Weight of precursor samples	21
Table IV.	Locations of samples while installed in the injection cage of the SAAL	22
Table V.	Properties of terrestrially prepared glasses	24
Table VI.	Crystalline phases identified by XRD in the calcia-gallia-silica (#2 and 4) and lead-silicate (#7) precursor samples	31
Table VII.	Visual observation of MEA/A-2 flight samples made immediately after removal from the SAAL	34
Table VIII.	Weight of MEA/A-2 samples	37
Table IX.	Important general results for MEA/A-2 experiment, STS-61A	40
Table X.	Relative wt% composition of the external surface of sample #2, MEA/A-2	50
Table XI.	Relative wt% composition in the interior of sample #2, MEA/A-2	53
Table XII.	Results for the hot pressed calcia-gallia-silica sample (#2) processed on MEA/A-2	59
Table XIII.	Results for the soda-lime-silica shell (#3) processed on MEA/A-2	62
Table XIV.	Refractive index, dispersion, and Abbe number for the 35.7 CaO-39.3 Ga_2O_3-25 SiO_2, mol%, glass melted in space (MEA/A-2) and on earth	64

EXECUTIVE SUMMARY

This report describes Experiment 81F01, "Containerless Processing of Glass Forming Melts in Space", NASA Contract NAS 8-34758. The experiment was conducted on 31 October 1985 in the MEA/A-2 on the D-1 Space Lab Mission of the Challenger space shuttle. Mission STS-61A was launched on 30 October 1985 from Cape Canaveral, Florida and landed on 6 November 1985 at Edwards Air Force Base, California.

The general plan of Experiment 81F01 was to heat, melt, and quench six spherical samples (~6 ± 1 mm in diameter) of different glass forming compositions while they were levitated in a single axis acoustic levitator furnace (SAAL). In addition, two non-melting sintered alumina (Al_2O_3) samples were used to check the operational characteristics of the SAAL under reduced gravity conditions. The flight hardware consisted of a furnace heated with four electrical resistance elements, a single axis acoustic levitator for holding the sample at a fixed position in the furnace, a sample insertion (into the furnace) and a retrieval mechanism, and a motion picture camera for photographing the samples while they were levitated in the hot furnace.

Three of the eight samples were levitated between 1250 and 1500°C before the lack of coolant created an over-temperature condition that caused the SAAL to shut down prematurely. Two of the three samples processed were calcia-gallia-silica and soda-lime-silica glass forming compositions.

The following major results were obtained.

1. For the first time, liquid samples were successfully levitated in space at high temperatures (1250 to 1500°C) for a considerable period of time (6 to 10 min).
2. Two glass forming samples (calcia-gallia-silica and soda-lime-silica) were successfully melted and cooled to glass while levitated in space.

3. Evidence of a two to three times increase in the tendency for glass formation was obtained for the calcia-gallia-silica glass. The final glass appeared to be reasonably homogeneous even though it was made from hot pressed crystalline powders which initially contained deliberate heterogeneities composed of 100 to 300 micrometer silica particles.

4. The primary purpose of the soda-lime-silica glass sample which contained a gas bubble was to demonstrate the feasibility of reshaping a glass shell in microgravity. The bubble inside the melt escaped during remelting in space for reasons not clearly known at this time.

5. An excellent photographic record (movie) was obtained of the sample processing sequences in microgravity. The film clearly showed that the levitator/furnace operated correctly for the first three samples. The quality of the film data is the best obtained to date and will provide valuable information for improving the positional stability of levitated samples at temperatures above 1250°C.

The pre- and post-flight handling and storage of the samples appears satisfactory. However, there is strong evidence that at least one of the molten samples was contaminated by the furnace insulation and perhaps other sources while it was levitated at elevated temperatures in the SAAL.

Only a portion of the scientific objectives of this experiment were met from the standpoint of glass formation and crystallization. The documented demonstration of levitating millimeter size liquid samples at temperatures above 1250°C for several minutes is viewed as a major advance in the practice of containerless materials processing in space.

I. INTRODUCTION

. Rationale for Processing Glass in Space

Glass melting in microgravity offers several advantages compared to melting on earth;[1-6] namely, (a) no container is necessary to hold the melt, and (b) the reduction (or absence) of convection and density driven segregation in fluid melts. On earth, heterogeneous nucleation/crystallization commonly occurs at the melt/container interface and this can prevent potentially useful compositions from forming glass. Potentially, this unwanted crystallization may be avoided or minimized by containerless processing, thereby, extending the compositional range for glass formation. Limited evidence of enhanced glass formation has been provided by an experiment in micro-g on Ge-Sb-S glasses.[7] Because of the smaller number of nuclei in the glasses made in micro-g, they were reported[7] to be more resistant to bulk crystallization than identical samples prepared on earth. The elimination of container-induced contamination offers the additional possibility of preparing chemically ultrapure glasses in micro-g. Glasses whose melts are highly corrosive or which require very high melting temperatures (2500-3000°C) where unreactive container materials are not available, can be prepared by containerless processing without introducing any impurities.

The absence of buoyant forces in micro-g can be utilized to prepare glass shells of precise sphericity and uniform wall thickness for use in laser fusion technology. Finally, basic phenomena such as bulk diffusion,[8] chemical corrosion,[9] surface tension, bubble motion/ dissolution,[10,11] etc. can be studied in fluid melts in micro-g without the detrimental disturbance of gravity driven convection and segregation. On earth, this unwanted convection can make the investigation of such phenomena either difficult or impossible.

B. Objectives of the D-1, MEA/A-2 Experiment

The principal objectives of this experiment were to:

a) obtain quantitative evidence for the suppression of heterogeneous nucleation/crystallization (or increase in glass formation) in containerless melts in micro-g,

b) study melt homogenization in the absence of gravity driven convection,

c) determine the feasibility of reshaping a glass shell in micro-g for use as a laser fusion target,

d) evaluate the procedures for preparing precursor samples that will yield bubble-free, high purity, chemically homogeneous melts in micro-g,

e) perform comparative property analysis of glasses melted on earth and in micro-g, and

f) assess the suitability of the single axis acoustic levitator/furnace for processing multicomponent, glass forming melts in micro-g.

Eight spherical samples (~6 ± 1 mm diameter), each with one or more of the above objectives, were to be processed at temperatures ranging from 900 to 1500°C for about 5 to 12 min in the single axis acoustic levitator (SAAL).* The sample composition, the detailed purpose of each sample, and the order and time-temperature for processing are given in Table I.

The suppression or reduction of heterogeneous nucleation/crystallization, the direct consequence of which is an increase in the compositional limits for glass formation, was to be studied by the containerless melting and cooling of compositions having different critical cooling rates. The critical cooling rate, R_c, is defined as the slowest rate at which a melt can be cooled without crystallizing (i.e., slowest cooling rate that will yield a glass). The

*Manufactured by Intersonics, Inc., Northbrook, IL.

TABLE I. Sample processing order, precursor description, and time line for MEA/A-2 Experiment 81F01. Conducted on STS-61A, 31 October 1985.

Sample Order	Precursor Composition (mol%) and Description	Purpose	Time-Temperature Profile	Time (min)	Elapsed Time (min)
			Preheat furnace to 1400°C	12	12
1	Alumina, high density	1. Operational check of levitator to confirm positioning and positioning stability. 2. Determine relative effects of acoustic streaming and positioning. Nonmelting sample is of comparable density to samples used on earth. 3. Confirm data from 1 g measurement.	Insert sample at 1400°C Hold at 1400°C Cool (no shroud) Retrieve sample	 3 2 	 17
			Preheat furnace to 1500°C	7	24
2	39.3 Ga_2O_3-35.7 CaO-25 SiO_2, sintered (hot pressed) compact	1. Operational check of levitator for liquid sample. 2. Evaluate improvement in homogeneity. 3. Assess precursor preparation procedures. 4. Comparative analysis with terrestrial sample.	Insert sample at 1500°C Hold at 1500°C Cool to ~700°C min. Retrieve sample	 4 4 	 32

TABLE I. (cont'd)

			Preheat furnace to 1250°C	5	37
3	Hollow glass shell (soda-lime)	1. Check of levitator for low density sample. 2. Evaluate bubble behavior. 3. Assess sample rotation.	Insert sample at 1250°C Hold at 1250°C Cool to ~600°C min. Retrieve sample	 2 10 	 49
		Rest period for cooling		180	229
			Preheat furnace to 1500°C	14	243
4	39.3 Ga_2O_3-35.7 CaO-25 SiO_2 glass containing colored dot marker (devitrified)	1. Operational check of levitator for liquid sample. 2. Determine extent of mixing in melt. 3. Assess precursor preparation procedures. 4. Acquire evidence of temperature gradients (Marangoni flow) in melt.	Insert sample at 1500°C Hold at 1500°C Insert cooling shroud Cool to ~700°C min. Retrieve sample	 4 3 	 250
			Preheat furnace to 900°C	5	255
5	33.3 Na_2O-66.7 B_2O_3 glass containing gas bubbles	1. Acquire data for bubble behavior (movement, dissolution/growth, nucleation, coalescence). 2. Assess sample rotation. 3. Comparative property analysis.	Insert sample at 900°C Hold at 900°C Cool to ~500°C Retrieve sample	 5 7 	 267

TABLE I. (cont'd)

		Rest period for cooling		180	447
			Preheat furnace to 1500°C	14	461
6	56 Ga_2O_3-44 CaO, devitrified	1. Critical cooling rate sample for evaluation of enhanced glass formation. 2. Comparative property analysis with terrestrially prepared sample.	Insert sample at 1500°C Hold at 1500°C Insert cooling shroud Cool to ≈700°C Retrieve sample	4 3	 468
			Preheat furnace to 900°C	5	473
7	50 PbO-50 SiO_2 sintered (hot pressed) compact	1. Operational check of levitator for liquid sample. 2. Evaluate improvement in homogeneity and possible mixing in melt. 3. Assess precursor preparation procedures. 4. Comparative property analysis with terrestrial sample.	Insert sample at 900°C Hold at 900°C Insert delayed cooling shroud Cool to ≈500°C Retrieve sample	5 7	 485
8	Alumina, low density	1. Operational check of levitator--prolonged levitation.			
		Apparatus shut down at ≈600 min from start			

volume fraction, V_c/V, crystallized in a material is dependent[12-14] on (a) the nucleation frequency, I, and crystal growth rate, U, which are functions of temperature, T, and (b) the time, t, at a particular temperature:

$$V_c/V = \pi/3\ I(T)\ U^3(T)\ t^4 \qquad (1)$$

The material is considered a glass when the volume fraction crystallized is below the detectable limit, i.e., $V_c/V < 10^{-6}$. The combined temperature dependence of I and U results in a nose shaped curve on a temperature-time (T-t) plot, Fig. 1. Such a curve is characteristic of a particular system, and is known as a time-temperature-transformation (TTT) diagram. T_n and t_n in Fig. 1 are the nose temperature and nose time, respectively. An approximate R_c derived from this curve is[15]

$$R_c = dT/dt = (T_m - T_n)/t_n \qquad (2)$$

where T_m is the liquidus temperature. Eq. (2) describes the slope of the line originating at the liquidus temperature and which just touches the nose of the TTT diagram. The ratio $R_c/R > 1$ is the criterion for crystallization and $R_c/R < 1$ is the condition for glass formation, where R is the rate of cooling the melt. When the thermal conductivity of the material is known, the critical maximum size of a sample obtainable as glass can also be derived.[16]

If I in Eq. (1) is significantly larger for heterogeneous nucleation, then the nose shaped curve is shifted to shorter times. Thus, the critical cooling rate is increased and the maximum sample size obtainable as glass is smaller. On the other hand, if heterogeneous nucleation caused by a container is absent in containerless melts in micro-g, then it should be possible to quench such melts to glass in space at cooling rates which are less than R_c on earth. Thus, the ratio of R_c (earth) to R_s (shuttle) for melts quenched to glass in micro-g should exceed unity and the numerical value of this ratio can be used as a quantitative measure of the degree to which glass formation is enhanced, or conversely, heterogeneous nucleation/crystallization is

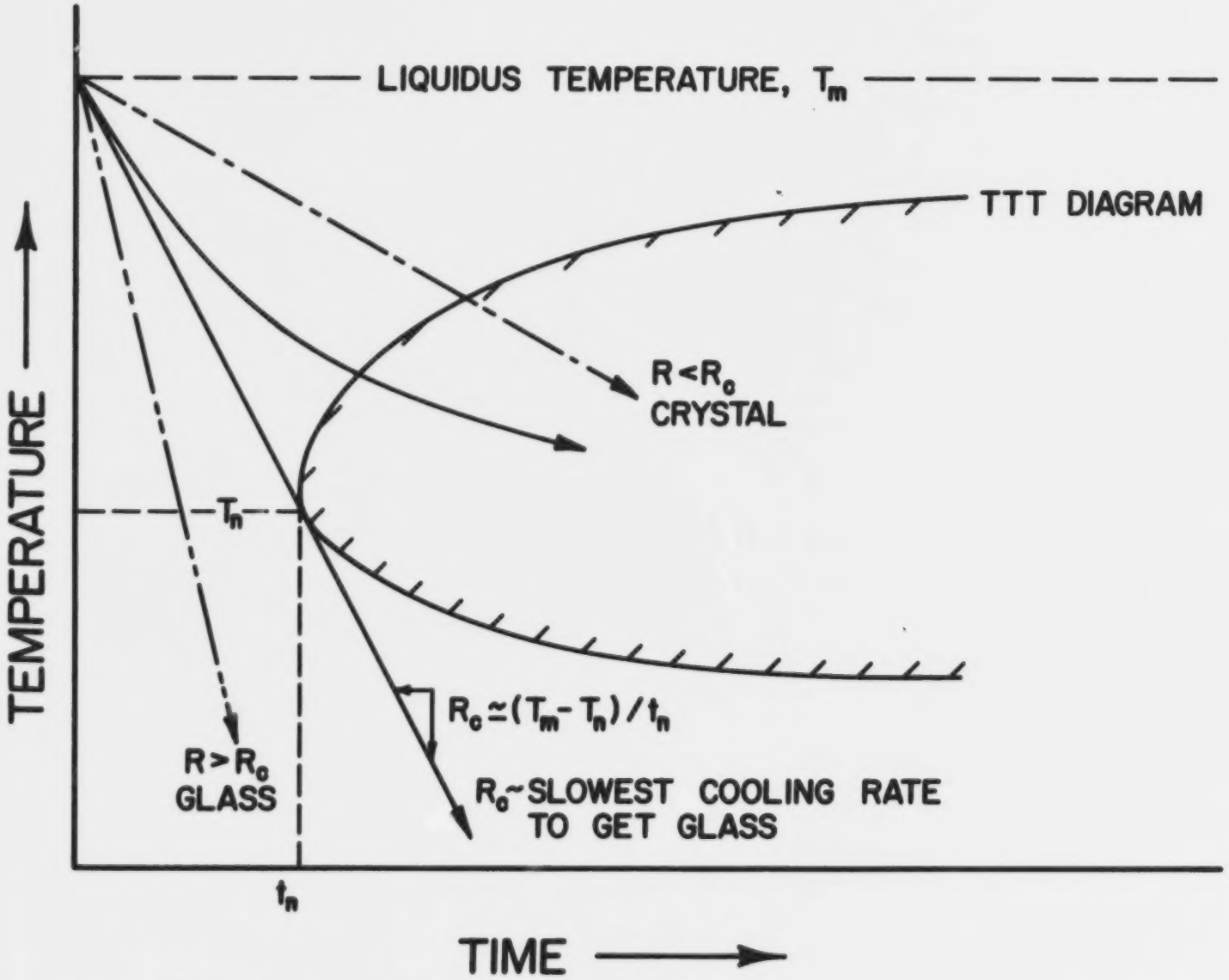

Figure 1. Typical time-temperature-transformation (TTT) diagram for a glass forming material showing critical cooling rate (R_c) for glass formation.

suppressed in containerless melts. The purpose of samples 2 and 6 (Table I), whose R_c on earth is 3 and 100 times higher than the cooling rate of the furnace used in micro-g (≈5°C/s) was to provide evidence for enhanced glass formation in micro-g.

Melt homogenization in the absence of gravity-driven convection in micro-g was to be investigated by observing the level of homogeneity achieved in precursor samples made with known chemical inhomogeneities. Sample 4, which contained a colored spot on its external surface, and samples 2 and 7 which were hot pressed samples containing relatively large SiO_2 particles (100 to 300 μm) were used for this purpose. The purpose of the sodium-borate sample (#5) was to provide information for the behavior of gas bubbles in liquid melts and supplemental data for melt homogenization in micro-g.

Glass shells several millimeters in diameter have important applications in laser fusion technology, but are essentially impossible to fabricate on earth. As there is no buoyant force in microgravity, a bubble initially present inside a glass shell should not necessarily escape when the glass is remelted in space. When remelting is performed without a container, surface tension forces should reshape the sample into a spherical shell of uniform wall thickness. A soda-lime-silica glass (sample #3 in Table I) containing an air bubble ≈3.75 mm in diameter was used for this purpose. Lastly, a wide range of physical, optical, thermal, and mechanical properties for glasses made in micro-g were to be compared with the same properties measured for glasses of identical composition made on earth.

There was no special basis for the different compositions used for this experiment. The ternary calcia-gallia-silica composition (samples 2 and 4) was chosen primarily because of its prior use in glass melting experiments in space, SPAR VI[17] and VIII[18] and STS-7 MEA/A-1.[19] Lead-silicate (sample #7) glasses are widely used on earth as commercial optical glasses, the large

difference in density between PbO and SiO_2 causes segregation of the melts on earth, and relevant property data are available. The binary calcia-gallia composition (#6) has a high critical cooling rate (550°C/s) and potentially interesting optical properties.

An important practical objective of this experiment was to determine the suitability of hot pressed, precursor samples for use in containerless melting. Precursor samples made by sintering/hot pressing have the advantage of being easily prepared without contamination from a container. A large sample can be hot pressed, with only the uncontaminated core being used for an experiment in space. It was of interest to determine the size of chemical inhomogeneities that can be tolerated in a hot pressed precursor which would yield a chemically homogeneous, multicomponent melt in a reasonable time when melted in micro-g.

II. PREPARATION AND HANDLING OF PRECURSOR SAMPLES

Of the eight samples in this experiment, four (#2, 4, 6, and 7) were prepared at the University of Missouri-Rolla. Samples 3 and 5 were supplied by Los Alamos National Laboratories (LANL) and Dr. S. Subramanian of Clarkson College, NY, respectively. The alumina samples 1 and 8, which were used primarily for the engineering check out of the SAAL, were supplied by Intersonics.

A. Sample #2

Sample 2 was a hot pressed 35.7 CaO-39.3 Ga_2O_3-25 SiO_2, mol% composition. The appropriate proportions of Ga_2O_3 (electronic grade, purity 99.999%)*, $CaCO_3$ (reagent grade), and -40 to +150 mesh (100 to 300 μm) crystalline silica

*Eagle-Picher Industries, Quapaw, OK, Lot A-420-1.

(quartz)* were first wet mixed (acetone). After drying, the mixture was tumbled for ~5 h. The powdered batch was cold pressed in a graphite mold at 140 x 10^4 kg/m^2 for 5 min and then hot pressed at 1130°C and 126 x 10^4 kg/m^2 for 8 h in an argon gas atmosphere. The hot pressed material was cooled slowly inside the graphite mold in flowing argon gas. After removing the hot pressed cylinder (~3.81 cm diameter and 2.52 cm long) from the graphite mold, it was heated at 1000°C for 6 h in air to burn out any carbon on its outer surface. To avoid contamination, the outer surface of the hot pressed cylinder which contacted the graphite mold was discarded. Spherical samples ~6 mm in diameter were ground by hand from the interior of the hot pressed cylinder. The spherical samples were washed with acetone in an ultrasonic cleaner, heated at 900°C for 20 h in flowing oxygen and then stored in a vacuum desiccator.

B. Sample #3

This sample was a soda-lime-silica glass sphere containing an air bubble. It was blown under reduced pressure (~30 cm of Hg) from a Kimble R-6 glass tube of 6 mm o.d. and 4 mm i.d. and was annealed in an open flame. The sample was lapped on a 3-point lapping machine using a diamond slurry as the grinding media and finally polished on a felt belt. After measuring its dimensions, weight and taking photographs from different directions, the sample was stored in an evacuated glass tube. Prior to sealing, X-radiographs of the shell were taken from different directions to determine the precise dimensions of the bubble and the wall thickness of the shell.

---

*Partiglo 280 Crystalline Quartz, Partiglo Processing and Classifying Corp., Paterson, NJ.

C. Sample #4

This sample was made from a 35.7 CaO-39.3 Ga_2O_3-25 SiO_2, mol%, glass which had been melted in a platinum crucible at 1500°C. The melt was stirred 5 times with a silica rod at 15 min intervals to ensure good chemical homogeneity. After the final stirring, the melt was held in the furnace (at 1500°C) for 15 min, cooled to 1450°C and held at this temperature for 1 h, and then cast into a preheated (500°C) graphite mold having four spherical (~7 mm diameter) cavities. A loaf casting (rectangular bar) was also made from the same melt and this glass was used for ground based property measurements. After cutting off the casting stem, the glass spheres were annealed at 600°C and cleaned with acetone. Previously prepared glass beads (~1 to 2 mm diameter) of the same overall composition, but colored with 3 wt% CoO, were fused onto each sphere using a spot heater. The colored beads were prepared by melting the cobalt oxide containing glass in the same way as described above and then pouring a stream of the melt onto a clean stainless steel plate from a height of 4 ft. Numerous small spheres <2 mm diameter formed from the splattered stream. The samples with the colored beads fused on their surface were cleaned with acetone in ultrasonic cleaner, devitrified by heating at 1000°C for one hour and stored in a vacuum desiccator.

D. Sample #5

Sample 5 was prepared from borax powder, which had been dried in a vacuum oven at 250°C for ~30 h, and which was melted in a platinum crucible at 1050°C. The melt was removed from the furnace and stirred vigorously with a platinum wire to entrap air bubbles. Small quantities of the melt were then poured directly into a 350 CS Dow-Corning silicone oil bath from a height of ~8 ft. Several nearly spherical samples containing one or more air bubbles of different size were obtained. The samples with the best bubble distribution were selected for the flight experiment. They were washed in amyl acetate

followed by acetone, dried, annealed at 390°C for 15 min and stored in a vacuum desiccator. Dr. S. Subramanian of Clarkson University was responsible for the preparation of sample 5.

E. Sample #6

A 56 Ga_2O_3-44 CaO, mol%, glass was melted in a platinum crucible at 1500°C for 45 min and stirred several times with a silica rod. This is a fluid melt at 1500°C with an estimated viscosity of <10 poise. Before casting, the melt was cooled to 1450°C and then cast into water at 27°C. The roughly spherical glass pieces obtained by water quenching were annealed at 700°C to remove internal stress, cooled to room temperature, cleaned with acetone, and then stored in a vacuum desiccator.

F. Sample #7

This sample was prepared by hot pressing a mixture of PbO (reagent grade)* and crystalline SiO_2 (quartz)** at 550°C and 105 x 10^4 kg/m^2 for 4 h in the same way as used for sample 4. The hand ground spherical samples were cleaned with acetone in an ultrasonic cleaner, heated at 600°C for 24 h in flowing oxygen and then stored in vacuum desiccator.

Before sending these precursor samples to the Marshall Space Flight Center (MSFC), they were photographed from different directions, weighed, and their dimensions measured. They were then sealed in evacuated (40-50 μm pressure) glass tubes. Figures 2 through 5 show the appearance of the precursors used for the D-1, MEA/A-2 experiment. The weight, average diameter, and bulk

---

*Fisher Scientific Company, Fair Lawn, NJ, Lot 740898.

**Partiglo 280 Crystalline Quartz, Partiglo Processing and Classifying Corp., Paterson, NJ.

OF POOR QUALITY

Figure 2. Hot pressed 35.7 CaO-39.3 Ga_2O_3-25 SiO_2, mol%, precursor sample (#2) used in D-1, MEA/A-2.

ORIGINAL PAGE IS
OF POOR QUALITY

Figure 3. Devitrified 35.7 CaO-39.3 Ga_2O_3-25 SiO_2, mol%, glass sample (#4) with colored spot used in D-1, MEA/A-2.

ORIGINAL PAGE IS
OF POOR QUALITY

Figure 4. Devitrified 44 CaO-56 Ga_2O_3, mol%, glass sample (#6) used in D-1, MEA/A-2.

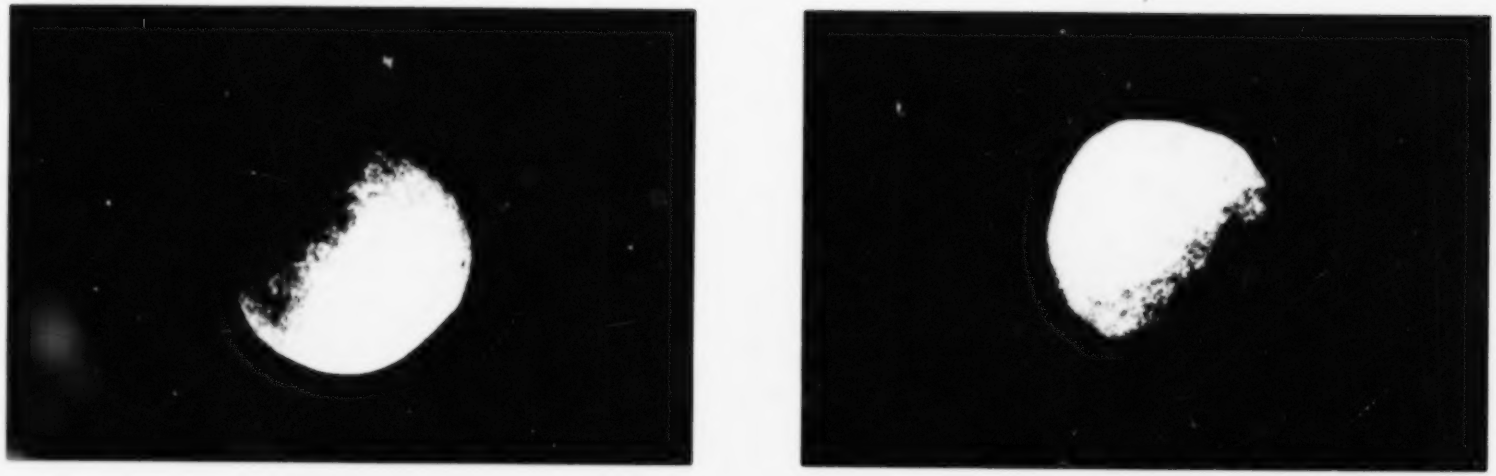

Figure 5. Hot pressed 50 PbO-50 SiO_2, mol%, sample (#7) used in D-1, MEA/A-2.

ORIGINAL PAGE IS
OF POOR QUALITY

density for each as-prepared precursor are given in Table II. Precautions were taken to avoid contaminating the samples and they were never touched with bare hands.

The precursor samples were hand carried to MSFC on 16 May 1985 for installation in the injection assemblies of the single axis acoustic levitator/furnace. The glass vial containing the primary precursor sample was broken and the weight of each precursor was measured in a dry box filled with dry argon (temperature 25 to 27°C, relative humidity <10%). A positive pressure of argon gas was maintained in the dry box to prevent any leakage of atmospheric air into the dry box. As shown by the weights in Table III, there was no detectable change in weight for any precursor during storage. After weighing, the precursor samples were installed in their respective injection cages, again in a dry box filled with dry argon. The injection cages were then installed in the levitator/furnace apparatus which was part of the MEA/A-2 equipment package. To minimize exposure of the samples to water vapor in the ambient atmosphere, the installation was done inside a plastic tent at 27°C and a relative humidity <15%.

It is to be noted that all the samples in Table I were installed in the injection cages on 28 June 1984 for the MEA/A-2 flight experiment which was then scheduled in October 1984. As this experiment was postponed, the samples were removed from the cages on 5 December 1984 and returned to the University of Missouri-Rolla (UMR) where they were stored in evacuated glass tubes. The samples were re-installed on 16 May 1985 for the MEA/A-2 flight experiment scheduled for October 1985. Each sample was examined and determined to be satisfactory for reuse. The position of each sample after installation in the injection cage was noted and is given in Table IV.

TABLE II. Initial weight, diameter, and density of precursor samples, as prepared.

	Sample Composition,* in mol%	Weight (gm) ± 0.0001	Average Diameter (mm)	Bulk Density (g/cm^3) ± 0.015
#2	39.3 Ga_2O_3-35.7 CaO-25 SiO_2 hot pressed, measured open porosity < 1%	0.5667	6.47 ± 0.015	4.016
#3	Soda-lime-silica, glass shell**	0.2000	5.780 ± 0.003	---
#4	39.3 Ga_2O_3-35.7 CaO-25 SiO_2 glass (devitrified) with blue dot	1.0515	7.77 ± 0.04	4.316
#5	33.3 Na_2O-66.7 B_2O_3 glass containing air bubbles***	0.3318	a) 6.72 ± 0.02 b) 5.73 ± 0.02 a ⊥ b	2.343
#6	56 Ga_2O_3-44 CaO glass devitrified	0.7660	a) 7.66 ± 0.015 b) 5.73 ± 0.015 a ⊥ b	4.430
#7	50 PbO-50 SiO_2 hot pressed, measured open porosity < 4%	1.0083	6.855 ± 0.015	5.93

*Samples 1 and 8 (alumina) were not measured.
**Measured at LANL.
***Measured at Clarkson College, NY.

TABLE III. Weight of precursor samples.

Sample No. for MEA/A-2 Experiment	Weight (gms) Measured at UMR*	Weight (gms) Measured at UMR on 4/16/85**	Weight (gms) Measured at MSFC on 5/16/85***
#2	0.5667 (3/8/84)	0.5669	0.5665
#3	0.2000 (2/24/84)	0.1809	0.1806
#4	1.0515 (8/28/82)	not measured	1.0515
#5	0.3318 (7/25/82)	not measured	0.3310
#6	0.7660 (8/28/82)	0.7664	0.7661
#7	1.0083 (3/8/84)	1.0012	1.0011
1 gm standard weight	1.0005	1.0003	1.0003

*Measured when the sample was originally prepared on the date in parentheses. Samples 3 and 5 were prepared and measured at Los Alamos National Laboratory and Clarkson College, NY, respectively.

**Measurements made to check the reusability of the samples in MEA/A-2.

***Date of installation in SAAL, MEA/A-2.

TABLE IV. Location of samples while installed in the injection cage of the SAAL.

NOTE: The injection/insertion assembly consists of a platinum wire cage at the bottom of which are located, in a rectangular pattern, four small pieces of alumina tubing which covers the platinum wire and which are in direct contact with the sample. The whole cage is fastened to a nearly cylindrical refractory material. A hollow alumina rod, which holds the sample tightly against the four small alumina pieces, can be moved in and out of this refractory material by means of a lever. The operating system of the lever is mounted at the top of the cage and the operation can be performed manually by nuts and screws located, if viewed from the front, on the left side of the cage. For this reference and description, this side will be called the "lever side". In the shuttle flight, the operation of this lever is fully automated.

Sample Number	Sample Location in the Injection Cage
#2 (hot pressed gallia-calcia-silica)	The sample was clamped so that the apex of two alumina pieces pointing toward the "lever side" of the injection cage was closer to the sample than the opposite apex formed by the other two alumina pieces.
#3 (soda-lime glass shell)	Spherical sample and positioned perfectly. No special orientation could be seen when viewed from any side of the cage.
#4 (devitrified gallia-calcia-silica sphere with blue dot)	The colored mark on the sample was positioned vertically upward. The hollow alumina tube covered the mark when the sample was clamped and the mark could not be seen visually.
#5 (borate glass with air bubbles)	The apex of two alumina pieces pointing opposite to the "lever side" was closer to the sample. The bubbles in the sample were concentrated toward the "lever side" of the cage.
#6 (devitrified gallia-calcia)	This sample was not perfectly spherical. The elliptical cross section (relatively flat surface) was placed on the horizontal plane.
#7 (hot pressed lead silicate)	The sample looked displaced a little with respect to the holding alumina tube toward the back of the cage while looking from the side.

III. PROPERTY ANALYSIS OF TERRESTRIALLY PREPARED SAMPLES

A sizeable quantity of the same material from which each precursor sample was prepared, was used to measure different physical, thermal and optical properties for comparison with the properties of the flight sample. The properties measured for the 35.7 CaO-39.3 Ga_2O_3-25 SiO_2 and 44 CaO-56 Ga_2O_3, mol% glasses are listed in Table V. The properties of the lead-silicate glasses are available in the literature and, therefore, were not measured at this time.

The critical cooling rate, R_c, for glass formation was determined by remelting a piece of glass on the tip of a thermocouple bead in a thermal image furnace and cooling it at different constant rates. The thermocouple output was connected to a calibrated strip chart recorder to obtain a temperature vs. time (cooling) curve for the sample. The slope of the cooling curve gives the rate of cooling. The minimum cooling rate for which the sample was totally glassy, as determined with an optical microscope at 40X, was taken as R_c. R_c determined in this way was also verified by constructing a TTT diagram for the glass. The temperature of the remelted sample on the thermocouple bead was quickly lowered to a temperature below the liquidus and held at that temperature until crystallization occurred. The time required to crystallize the sample at a particular temperature was plotted against temperature to obtain the nose shaped TTT diagram, as described in section IB. The R_c values determined by visual observation and TTT diagram were within ±1°C/s.

A typical experimentally determined TTT diagram for the 35.7 CaO-39.3 Ga_2O_3-25 SiO_2, mol%, glass for a sample diameter ≈3.5 mm is shown in Fig. 6. From this diagram, R_c is determined to be 3.2°C/s. For larger sample diameters, the cooling rate needed to obtain glass obviously increases as shown in Fig. 7. The ≈11.3°C/s cooling rate required to form glass for a sample of this melt whose size was identical to that used in the flight experiment (for

TABLE V. Properties of terrestrially prepared glasses.

	56 Ga_2O_3-44 CaO*	39.3 Ga_2O_3-35.7 CaO-25 SiO_2*
Number of Corresponding Sample in Table I	6	2 and 4
Bulk Density, D (g/cm^3)	4.480 ± 0.015	4.195 ± 0.015
Critical Cooling Rate, R_c (°C/s), for a sample ~6 mm in diameter	550 ± 50	11 ± 2
Crystallization Temp. T_x (°C)	775 ± 5	887 ± 5
Refractive Index, n_D	1.7985 ± 0.0008	1.7121 ± 0.0008
Dispersion, n_F-n_C	0.0290 ± 0.0015	0.0175 ± 0.0015
Abbe Number, ν	27.4 ± 2.5	40.5 ± 2.5

*Compositions are in mol%.

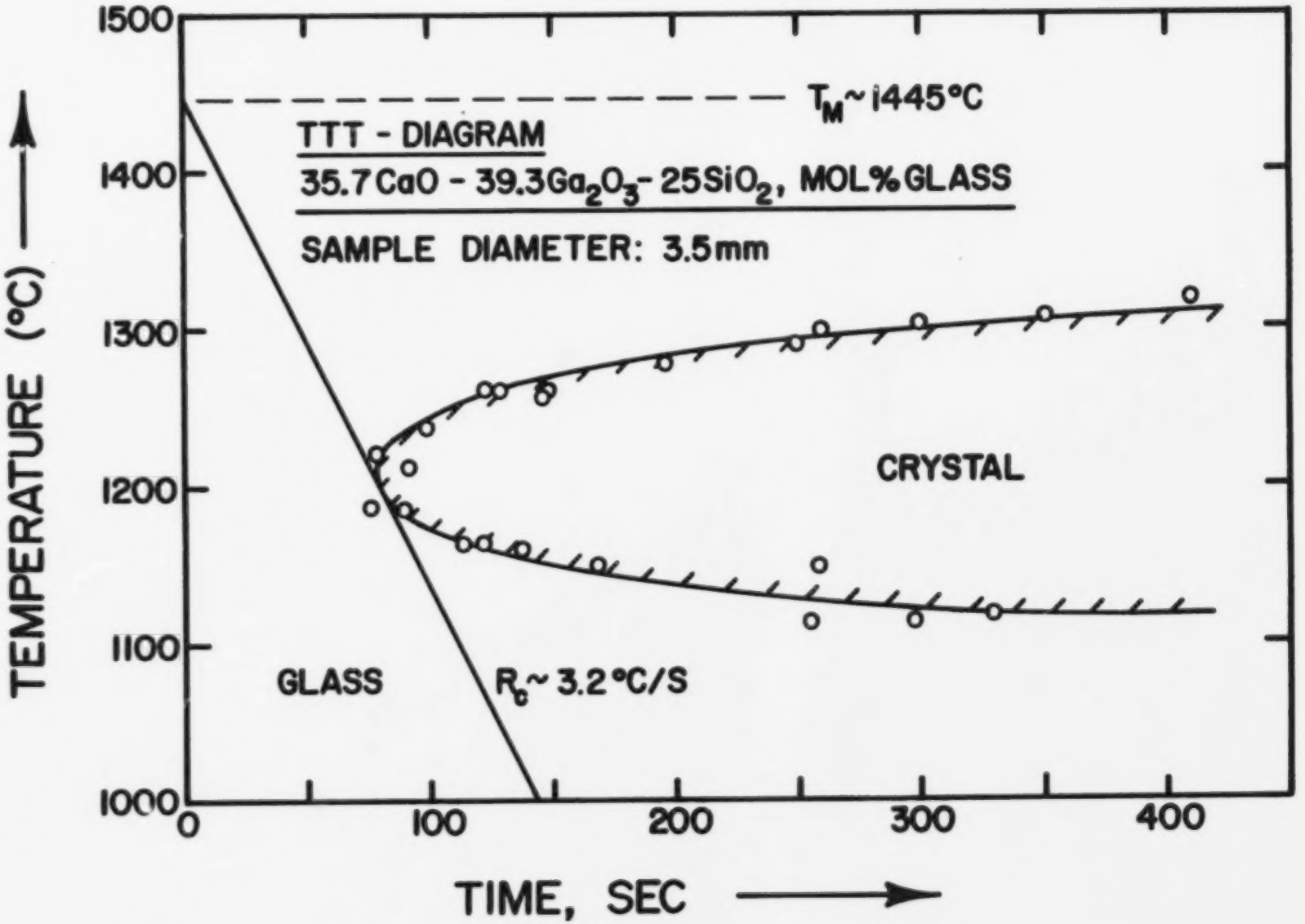

Figure 6. TTT diagram for the 35.7 CaO-39.3 Ga_2O_3-25 SiO_2, mol%, composition for sample diameter ~3.5 mm.

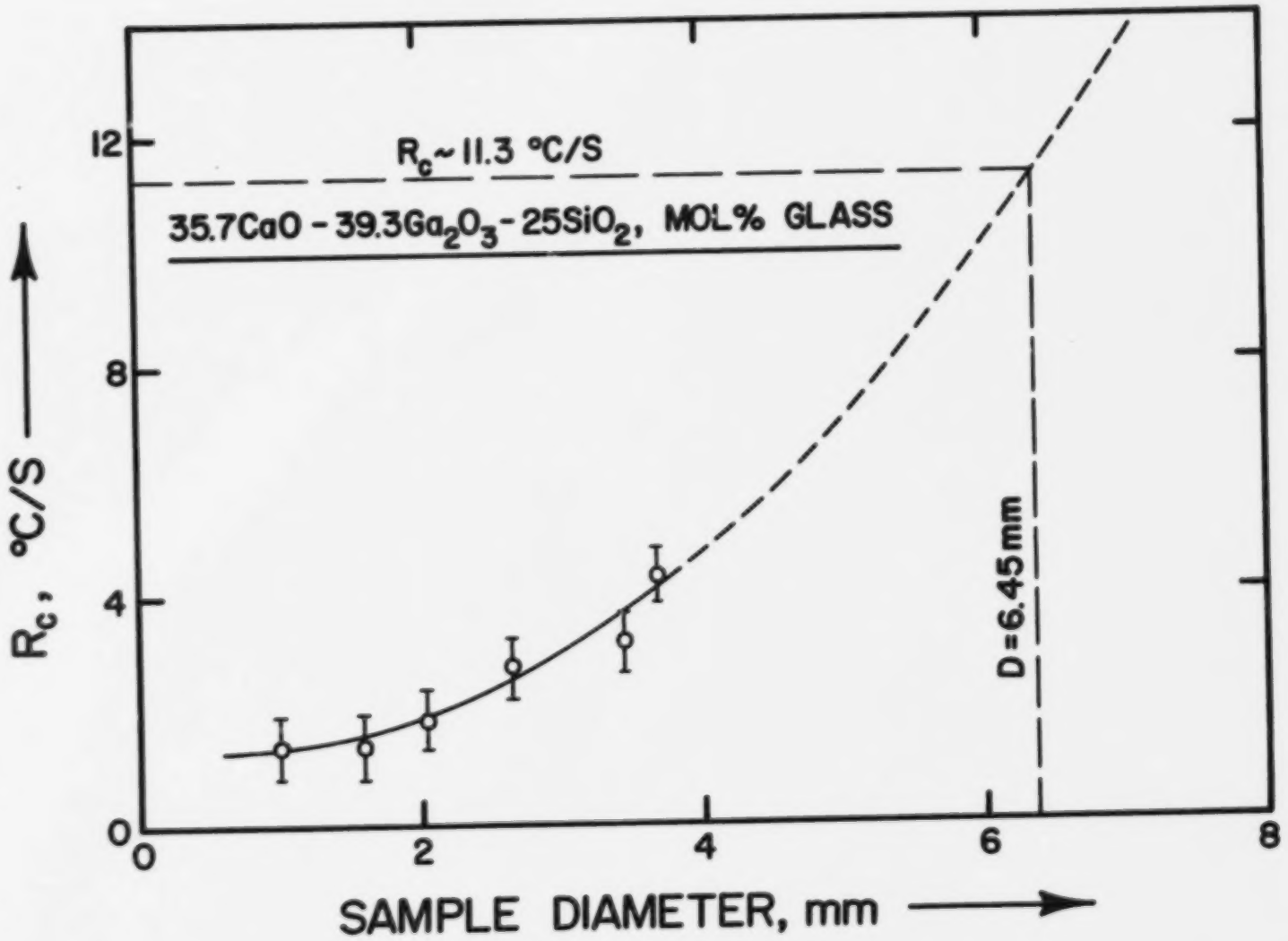

Figure 7. Dependence of the cooling rate measured on earth for glass formation upon sample diameter for the 35.7 CaO-39.3 Ga_2O_3-25 SiO_2, mol%, composition.

example sample #2, diameter 6.5 mm) was determined from extrapolation (Fig. 7). This value was determined by extrapolating the results for smaller samples because a liquid sample with diameter >4 mm would not adhere to the thermocouple bead because of its excessive weight on earth (in one-g).

The inhomogeneities present in the hot pressed precursor were characterized by examining a fracture surface with a scanning electron microscope (SEM). Figures 8 and 9 show the general appearance of the hot pressed calcia-gallia-silica sample (#2) and the presence of unreacted silica (quartz) particles of different size dispersed in the calcia-gallia matrix. The partial dissolution of the silica particles during hot pressing is also apparent in Fig. 9. A reaction layer ~10 to 20 μm around the silica particle is observed after hot pressing (1130°C and 1800 psi for 8 h in argon atmosphere). Unreacted silica particles are also visible in the fracture surface of the hot pressed lead-silicate sample (Fig. 10). X-ray diffraction (XRD) analysis of the hot pressed precursor showed that β-Ga_2O_3, $Ca_2Ga_2SiO_7$, $CaGa_2O_4$ and SiO_2, and $PbSiO_3$, Pb_2SiO_4 and SiO_2 were present in the calcia-gallia-silica and lead-silicate samples (Table VI), respectively. A small sample of the hot pressed material yielded a homogeneous glass, as determined by SEM, when it was given the thermal treatment planned for the flight experiment, i.e., 1500°C for 4 min for the calcia-gallia-silica sample and 900°C for 5 min for the lead-silicate sample (see Table I, samples 2 and 7). In contrast to the hot pressed samples, the devitrified glasses of the calcia-gallia-silica and lead-silicate compositions contained β-Ga_2O_3 and $Ca_2Ga_2SiO_7$, and $PbSiO_3$ and Pb_2SiO_4, respectively (Table VI).

ORIGINAL PAGE IS
OF POOR QUALITY

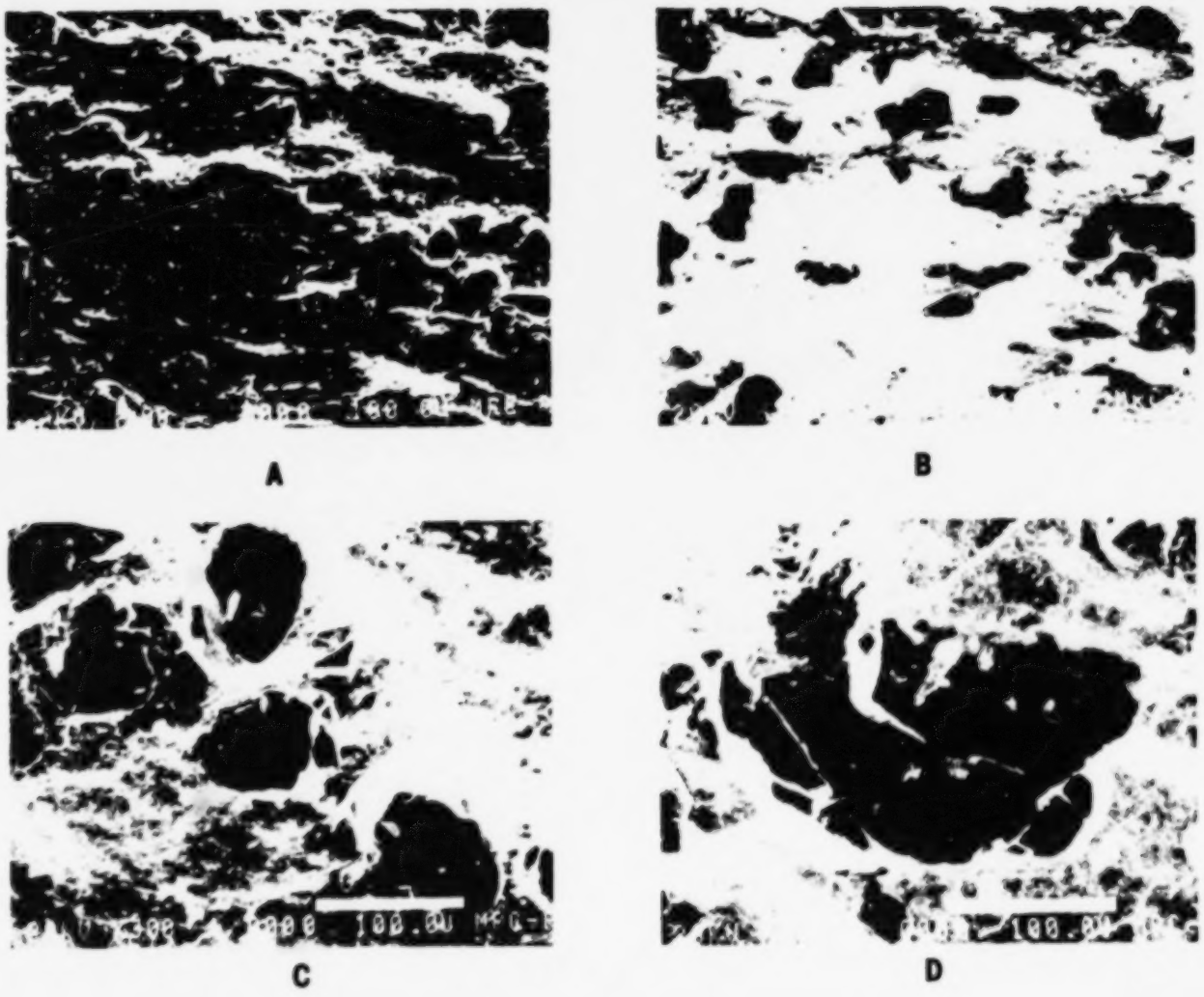

Figure 8. Appearance of the interior of the hot pressed 35.7 CaO-39.3 Ga_2O_3-25 SiO_2, mol%, precursor as seen by SEM. Dark regions are silica particles. B is the back scattered photograph of the sample shown in A. Figure C shows silica particles ~100 micrometer size while larger silica particles ~300 micrometer in size are shown in D.

ORIGINAL PAGE IS
OF POOR QUALITY

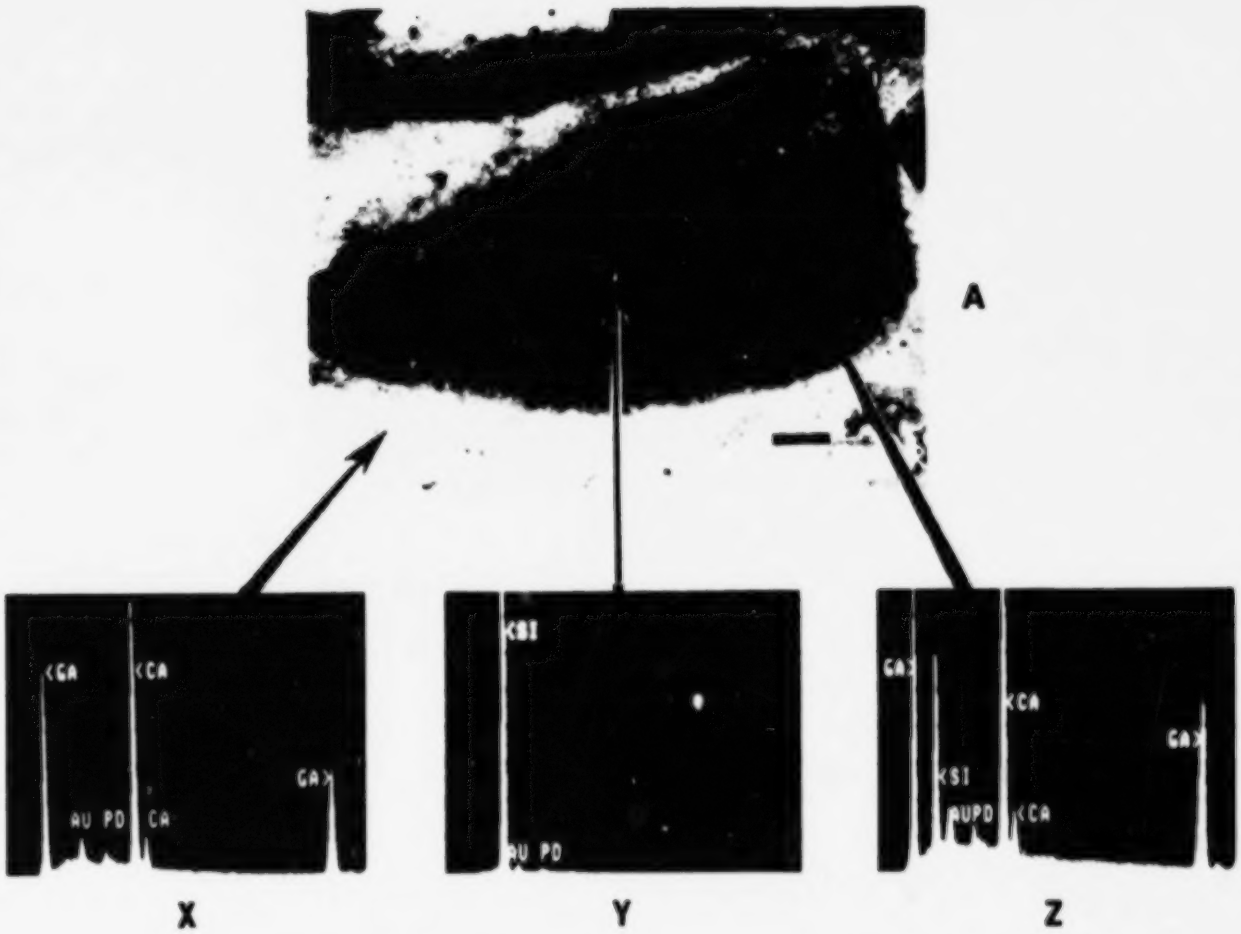

Figure 9. Magnified view of a silica particle in the fracture surface of the 35.7 CaO-39.3 Ga_2O_3-25 SiO_2, mol%, hot pressed precursor. The reaction of the silica particle with the calcia-gallia matrix produces the reaction zone shown in A. X, Y, Z show the elements found by EDAX in the calcia-gallia matrix, silica particle, and the reaction zone, respectively.

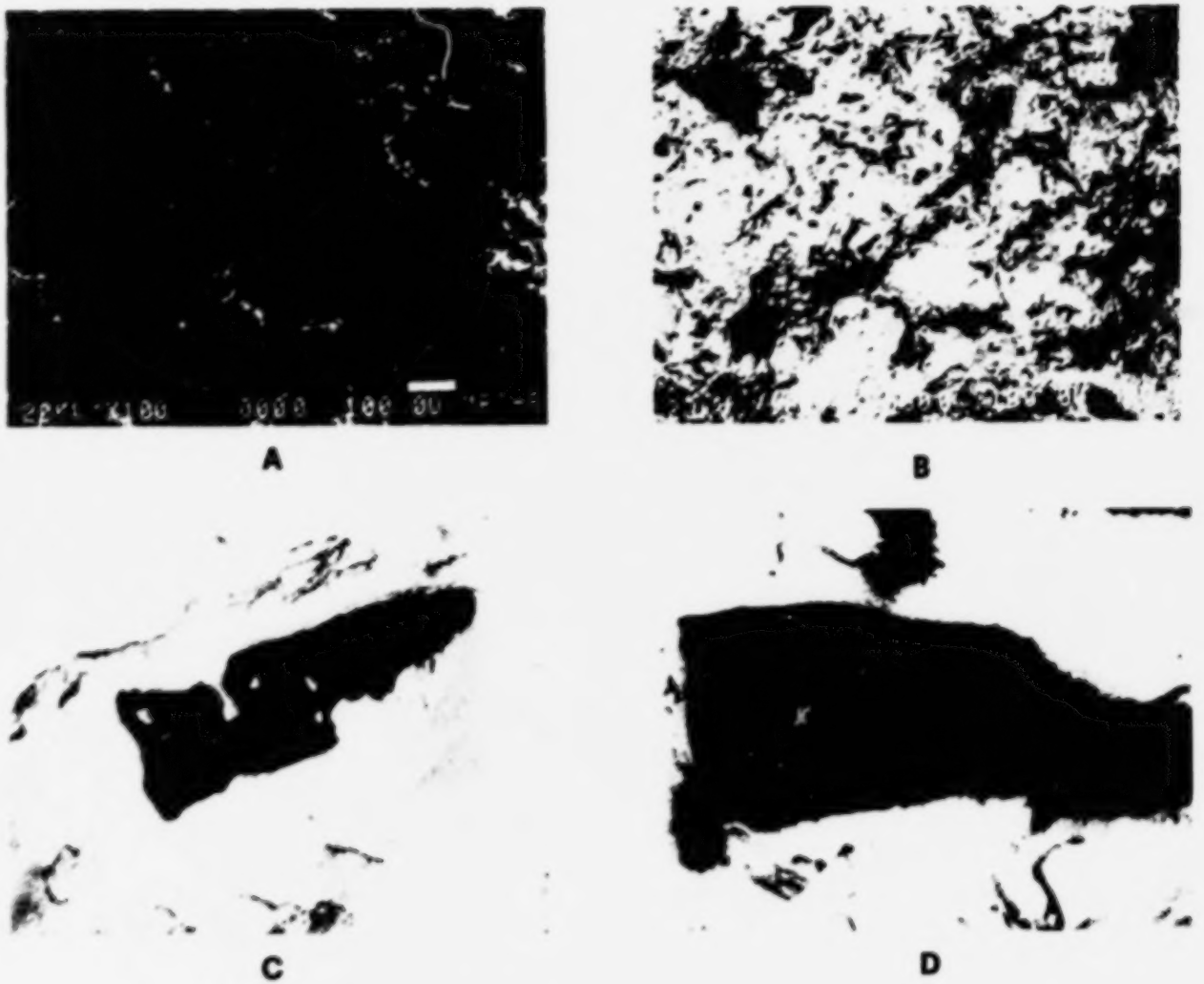

Figure 10. Appearance of the interior of the hot pressed 50 PbO-50 SiO_2, mol%, precursor as seen by SEM. B is the back scattered photograph of the region shown in A. C and D show magnified views of the silica particles in the matrix.

ORIGINAL PAGE IS
OF POOR QUALITY

TABLE VI. Crystalline phases identified by XRD in the calcia-gallia-silica (#2 and 4) and lead-silicate (#7) precursor samples.

Composition, Mol%	Sample Description	Crystalline Phases Identified
	Portion of hot pressed material from which precursor sample 2 was made.	β-Ga_2O_3, $CaGa_2O_4$, $Ca_2Ga_2SiO_7$, and SiO_2
39.3 Ga_2O_3-35.7 CaO-25 SiO_2	Glass sample devitrified at 1000°C for 1 h. Same heat treatment used for precursor sample 4.	β-Ga_2O_3 and $Ca_2Ga_2SiO_7$
	Portion of hot pressed material from which precursor sample 7 was prepared.	$PbSiO_3$, SiO_2, and Pb_2SiO_4
50 PbO-50 SiO_2	Glass sample devitrified at 600°C for 2 h.	$PbSiO_3$ and Pb_2SiO_4

IV. REMOVAL AND HANDLING OF POST-FLIGHT SAMPLES

When returned to MSFC, after the completion of the D-1 mission the entire MEA/A-2 flight apparatus was placed inside a plastic tent in a large dust-free room. The space under the tent was maintained at a temperature 27°C and a relative humidity of <15%. Preliminary examination of the acoustic levitator after the flight experiment showed that it was in good condition. The position of the carousel holding the sample injectors was between sample position numbers 1 and 2 with reference to the levitator/furnace.

The flight samples were removed from the MEA/A-2 flight apparatus on 2 December 1985 in consecutive numerical order starting with sample 1 and ending with sample 8. After detaching each sample injector from the SAAL, each injector holding a sample was sealed in a separate plastic container which had been previously purged with dry air. These plastic containers were then transferred to a glove box filled with dry argon gas (27°C, relative humidity <15%) for the purpose of removing the samples from the injection cages.

The samples (except #2) were removed from their cages on 3 December 1985 and stored temporarily in small plastic bags. The samples were handled with a clean plastic tube connected to a vacuum pump. Sample 2 (calcia-gallia-silica, hot pressed) was stuck to the platinum wire cage and could not be removed from the cage at that time. The entire cage along with the adhering sample (#2) was stored in a clean plastic bag containing a desiccant. The samples (except #2) were then weighed, photographed, and sealed in evacuated glass tubes. All the samples (except #3) were hand carried to the University of Missouri-Rolla, Materials Research Center, for analysis. Sample 3, which had been a hollow shell of soda-lime-silica glass, was transferred to Mr. Frank Gac who hand carried it to LANL. Three prints of the motion picture film from the flight experiment were given to D. E. Day and he transferred one copy to Frank Gac of LANL.

V. POST-FLIGHT SAMPLE ANALYSIS

A. Visual Examination

Immediately after removal from the MEA/A-2 hardware and SAAL at MSFC, each sample was visually examined and its position in the injection cage was compared with that as initially installed. The observations are given in Table VII. Samples 1 and 3 were found to be loose inside the platinum wire cage instead of being clamped between the cage and alumina tube. Sample 3 appeared to be totally glassy, but the bubble initially present inside this sample was not visible. Sample 2 was found stuck to one side of the cage at the junction of three platinum wires, see Figs. 11 and 12. All three wires were partially imbedded in the sample. That portion of the sample touching the cage wires was crystalline, but the remaining part was glassy. No change in color, shape, or position (compared to that as installed) was detectable for samples 4 through 8 and each of these samples was still clamped between the cage and alumina tube as when they were installed. Based on the location of samples 4 through 8 it appears that none of them had been inserted into the hot furnace, released, and levitated.

B. Weight Change

The weight of each sample was measured after the flight experiment and compared with its weight when installed (precursor samples) in the acoustic levitator/furnace, see Table VIII. Flight sample 2 could not be weighed as it had stuck to the cage. There was no known reason to expect a weight change for any of the samples melted in space and no experimentally significant weight change was observed. The weight of each sample remained constant for the period it was stored in the MEA/A-2 flight apparatus before and after the flight experiment.

TABLE VII. Visual observation of MEA/A-2 flight samples made immediately after removal from the SAAL-1 at MSFC on 2 December 1985.

Sample No. (for description see Table I)	Observations/Remarks
#1	Sample looks good. No change in color. Not clamped (captured) between the cage and alumina tube.
#2	Sample stuck to the platinum cage wires and located between the central thick horizontal wire, one thin and a thick vertical wire. All three platinum wires were partially embedded in the sample. The parts of the sample in contact with the wires were crystalline, whereas, the central portion (not in contact with the wires) is glassy.
#3	Glass sample. Looks spherical. The bubble originally present inside the sample was not visible. Not captured by the cage and alumina tube and found sitting loosely at the bottom of the cage.
#4	No change in color or shape. Sample looks good. Perfectly clamped between the cage and the alumina tube. Sample appears to be in the same position as when installed.
#5	No change in color or in shape. The position of the bubbles inside the sample appears unchanged. No positional change is evident when compared to installed position.
#6	No change in color, shape, or position.
#7	No change in color, shape, or position.
#8	No change in color, shape, or position.

ORIGINAL PAGE IS
OF POOR QUALITY

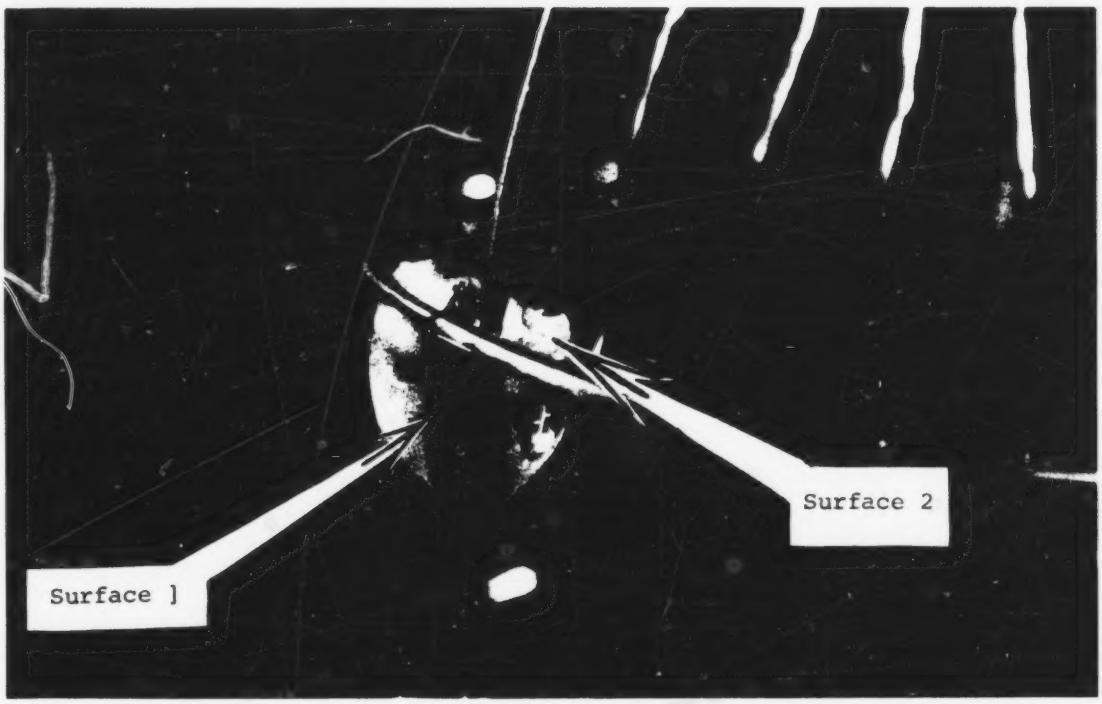

Figure 11. Flight sample 2 (35.7 CaO-39.3 Ga_2O_3-25 SiO_2, mol%, hot pressed) stuck to platinum wire cage while levitated and melted in space (MEA/A-2). The sample crystallized where it contacted the cage wires.

ORIGINAL PAGE IS
OF POOR QUALITY

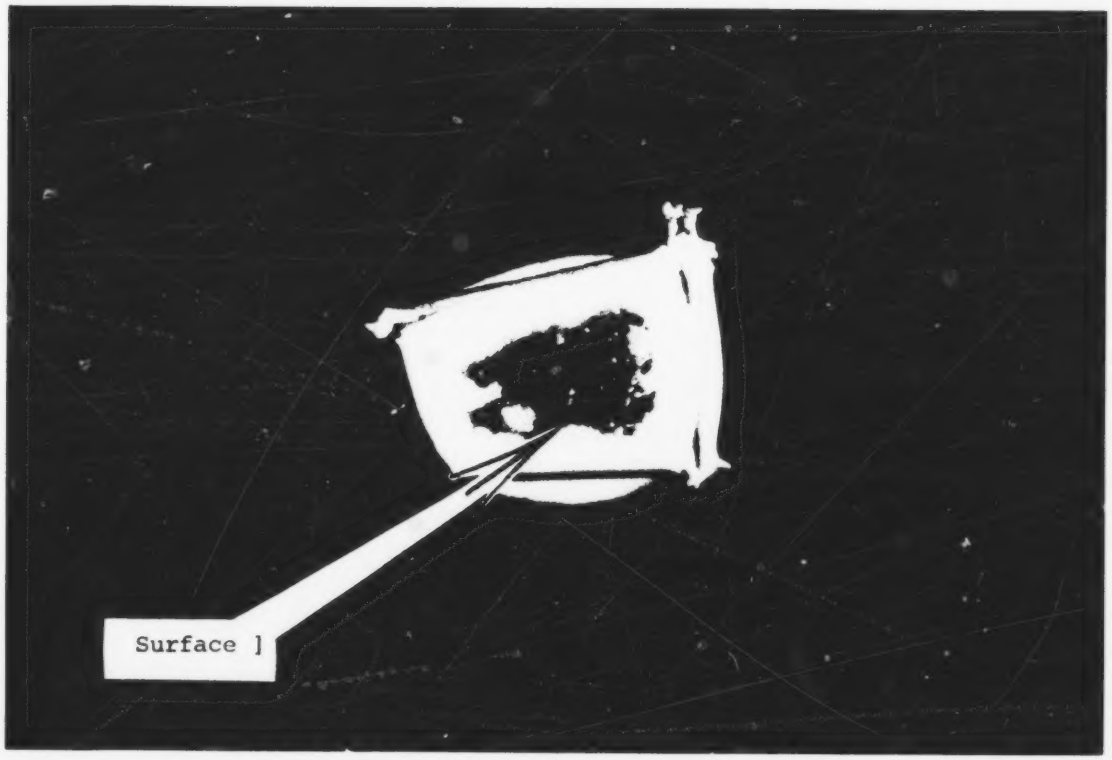

Figure 12. Flight sample 2 (35.7 CaO-39.3 Ga_2O_3-25 SiO_2, mol%, hot pressed), MEA/A-2, with the imbedded platinum wires.

TABLE VIII. Weight of MEA/A-2 samples.

Sample No. (for description see Table I)	Weight (gm) Flight Sample. Measured at MSFC on 12/3/85 after removal from the sample injectors.	Weight (gm) Precursor Sample. Measured at MSFC on 5/16/85 before installation in the injectors.	Difference (gm)
#1	0.5136	*	---
#2	**	0.5665	---
#3	0.1813	0.1806	+0.0007
#4	1.0511	1.0515	-0.0004
#5	0.3310	0.3310	0.0000
#6	0.7654	0.7661	-0.0007
#7	1.0013	1.0011	+0.0002
#8	0.0742	*	---
Standard Weight	1.0004	1.0003	+0.0001

*Alumina sample, not measured when installed.
**Flight sample #2 stuck to the cage and, therefore, was not measured after recovery.

C. Film and Flight Data

A motion picture camera recorded the sample while it was inside the SAAL. A photographic record was obtained for samples 1, 2, and 3 only and no data was obtained for the remaining five samples (#4 through 8). The film showed that the injection mechanism worked satisfactorily for all three samples. Immediately after release, the samples oscillated over a distance of roughly two sample diameters, but gradually became more stable with time. The samples oscillated with a simple harmonic motion for a few seconds in a plane perpendicular to the line joining the sound source and reflector after being inserted into the SAAL and released but did not touch the platinum cage. The magnitude of this oscillation gradually diminished until the sample became almost stationary in the acoustic energy well. The sample remained stationary even after becoming molten, but then started oscillating again when the cooling shroud gate opened. It was clear from the film that sample 2 struck and adhered to the platinum cage on the side opposite to the cooling shroud gate. The instability of sample 2 and its movement out of the acoustic well occurred at the time the shroud gate opened for cooling the sample. No specific reason is known for why sample 2 escaped from the acoustic energy well, but it is possible that a temperature gradient caused by opening the cooling shroud gate produced a large pressure gradient inside the furnace which was sufficient to destabilize and displace sample 2 from the acoustic energy well.

The bubble inside sample 3 appeared spherical and symmetrical with respect to the outer surface of the glass when the sample was fully molten. It remained like this for ≈75% of the time at maximum temperature. A few seconds before cooling commenced, the bubble started moving slowly to one side of the sample and eventually escaped from the sample just after cooling commenced.

The recapture of samples 1 and 3 by the cage and alumina tube and the retraction of the sample injector from the SAAL were not visible since the

illumination for filming was too low at the recapture temperature. The only illumination available is that from the heating elements. None of samples 1, 2, or 3 were found clamped between the cage and the alumina tube as planned for normal recovery. Based on visual observations and the film data, the overall results of the MEA/A-2 flight experiment are summarized in Table IX.

It should be noted that the temperature and time desired for processing samples 2 and 3 were not precisely maintained during the flight experiment and a random temperature fluctuation inside the furnace was also observed. The temperature-time profile actually followed for samples 2 and 3 is compared with the desired profile in Figs. 13 and 14, respectively. For sample 2, the furnace temperature was 1550°C instead of 1500°C just before sample insertion. During sample insertion the temperature dropped to 1450°C and remained there for 2 min 15 s. The original plan was to heat the sample at 1500°C for 4 min, but the sample was actually held at 1450°C for 2 min 15 s and at 1500°C for 1 min 45 s before cooling started. After cooling for 4 min the sample was retrieved from the furnace at 820°C instead of 700°C as desired. For sample 3, the furnace temperature was 90-100°C higher than the planned temperature of 1250°C (see Fig. 14) and the sample was retrieved at 500°C instead of 600°C.

D. Sample Analysis, Scanning Electron Microscopy (SEM)

Sample 1 and 8 (Alumina). When examined by SEM, numerous foreign particles were found on the surface of sample 1. When these particles were analyzed by energy dispersive x-ray analysis (EDAX), the elements Si, Mg, Ti, Ag, K, and Cl were detected. The surface of the other alumina sample (#8), which was not levitated or processed during the MEA/A-2 experiment was also examined by SEM and found to contain Si, K, and Cl. The source of this contamination on samples 1 and 8 is unknown.

Sample 2 (Calcia-Gallia-Silica, Hot-Pressed). This sample was removed from the platinum wire cage by cutting the wires to which it stuck, see Fig.

TABLE IX. Important general results for MEA/A-2 experiment, STS-61A.

1. Three samples were levitated and heat treated as planned.
2. The single axis acoustic levitator/furnace (SAAL) operated satisfactorily.
3. A fluid melt was successfully levitated at temperatures between 1250 and 1500°C for several minutes (6 to 10 min).
4. Two melts were successfully quenched to glass.
5. A good photographic record was obtained for the entire processing cycle of the three samples processed.
6. Hot pressing is a feasible means of preparing precursor samples.

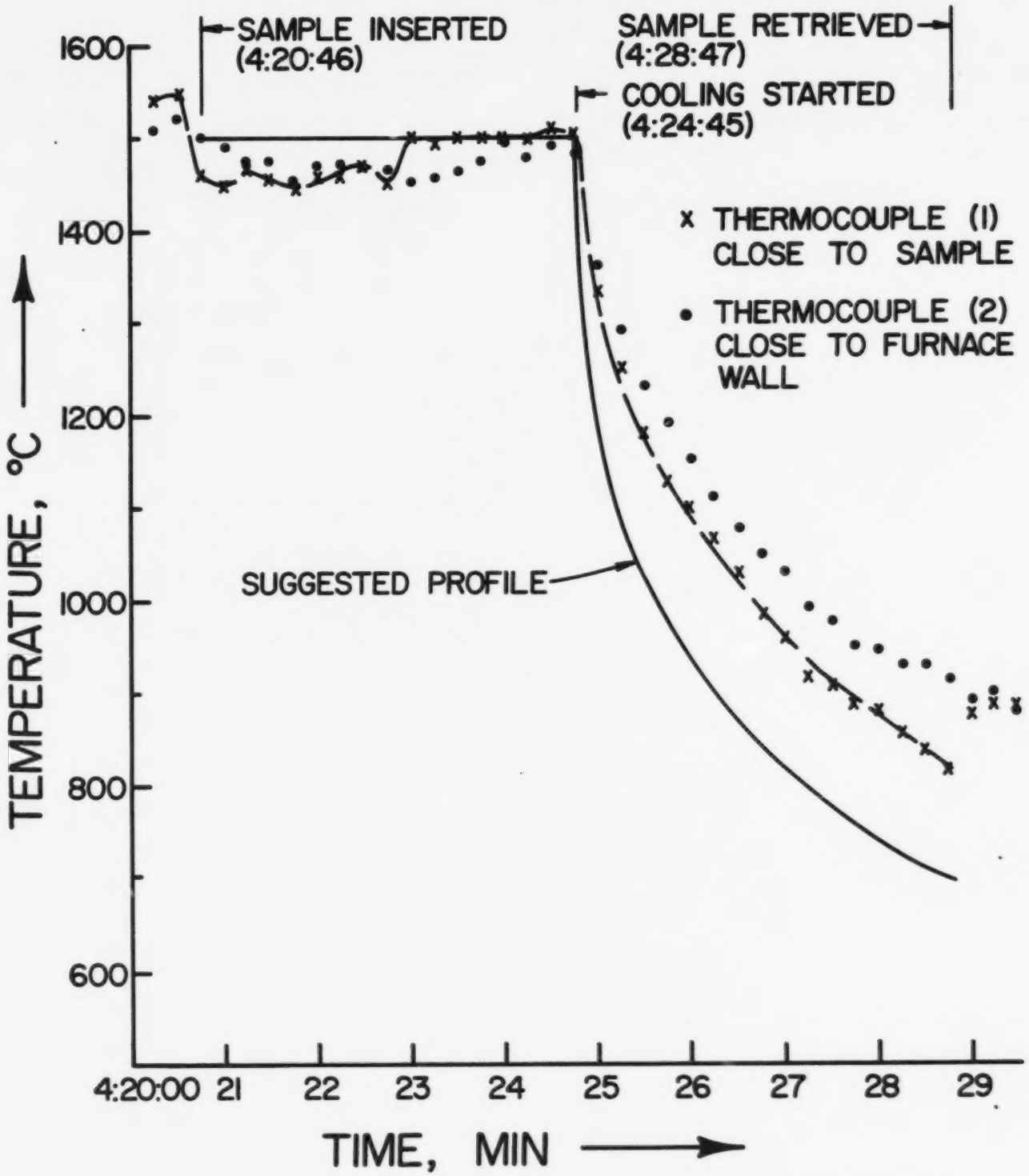

Figure 13. The planned and observed time-temperature profile for 35.7 CaO-39.3 Ga_2O_3-25 SiO_2, mol%, hot pressed sample (#2) when processed in the single axis acoustic levitator, MEA/A-2.

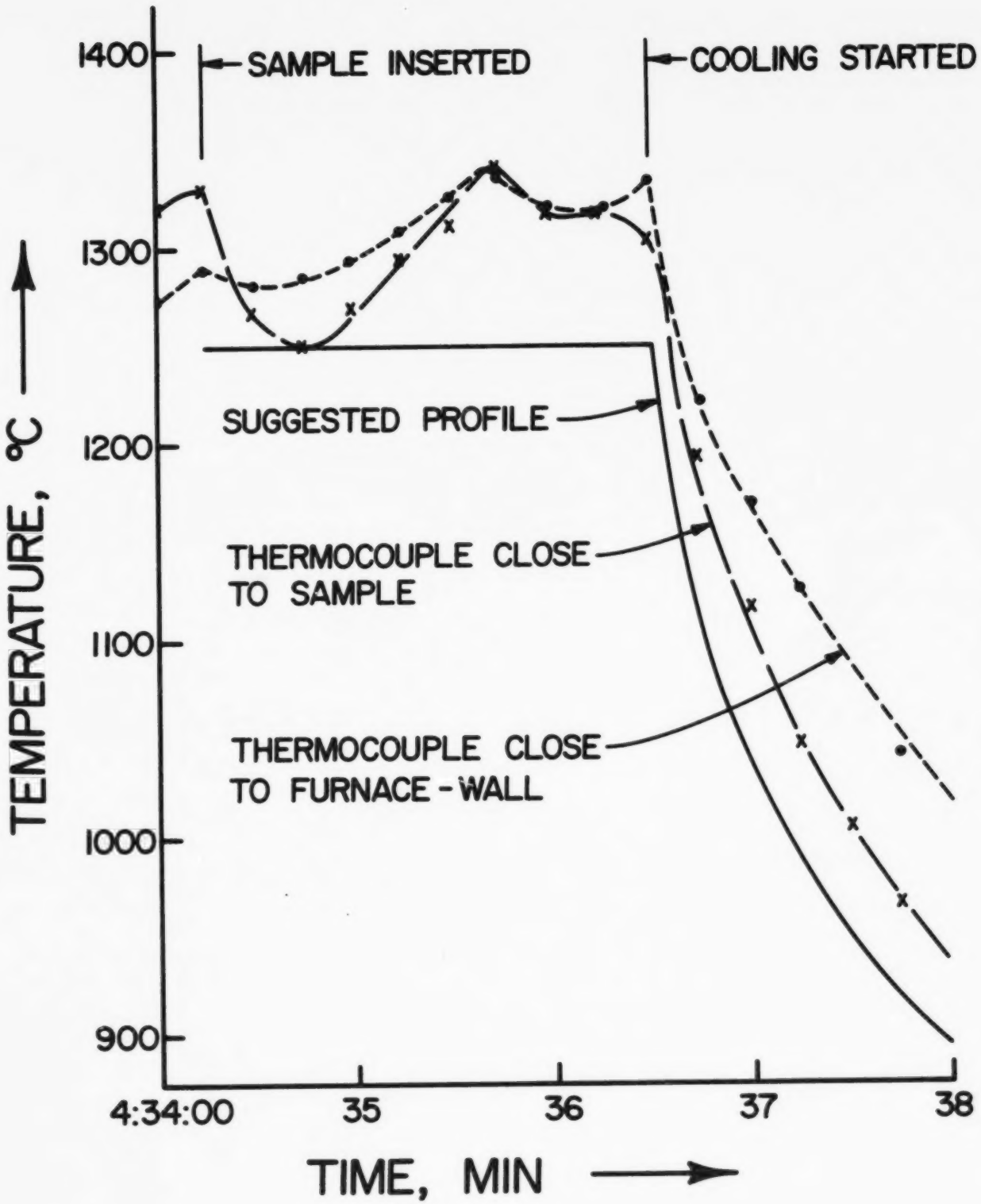

Figure 14. The planned and observed time-temperature profile for the soda-lime-silica glass shell (#3) processed in the acoustic levitator, MEA/A-2.

12. Figure 15 shows the sample when the platinum wires imbedded in the sample were removed. The sample was examined first with an optical microscope at 40x. That part of the sample touching the wires was crystallized for a distance of about 1 mm from both sides of the wire. The central part of this sample which did not touch the wires was glassy, with scattered crystals on the surface of the glassy portion. Crystallization on the surface opposite to the cage (surface 2, see Fig. 11), was considerably less than on the surface touching the cage (surface 1). Several small gas bubbles (≈20 to 30, diameter ≈0.17 mm and less) were also visible and they tended to concentrate toward the surface facing the tip of the platinum wire cage (i.e., in the direction of the sound source). When examined by SEM, two types of crystals, one flat and smooth and the other rough and needle shaped, were found on the external surface (Fig. 16). EDAX showed that the flat, smooth crystals contained primarily Ga while the rough crystals contained Ca, Ga, and Si. XRD analysis of the hot pressed material of this same calcia-gallia-silica composition, which had been melted and devitrified on earth, suggests that the crystals are β-Ga_2O_3 and $Ca_2Ga_2SiO_7$. The small quantity of crystals from the flight sample has prevented their positive XRD identification.

Numerous rod shaped particles (≈3 to 4 μm in diameter and 20 to 50 μm long), such as those shown in Fig. 17, were found at different locations on the platinum wires imbedded in flight sample 2. EDAX showed that these rods contained 70 to 80 wt% Al_2O_3 and 20 to 30 wt% SiO_2. This is very close to composition of mullite (wt% composition, 71.8 Al_2O_3-28.2 SiO_2). The surface of sample 2 was also found to be contaminated by these rod shaped particles and they could have initiated the scattered crystallization on the surface of sample 2 (Fig. 18). A piece of the refractory insulation used in the SAAL also contained particles whose size, shape, and chemical composition were identical with those found on the sample 2 (Fig. 17). The extraneous

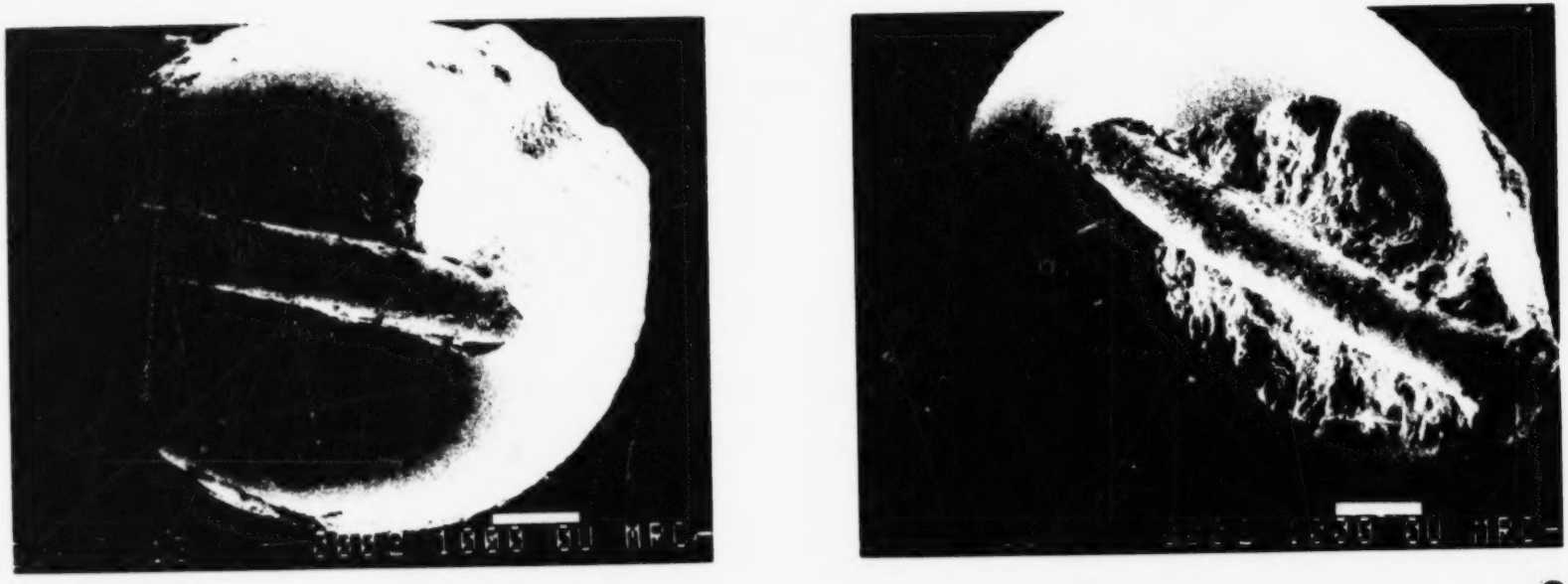

Figure 15. Appearance of flight sample 2 (35.7 CaO-39.3 Ga_2O_3-25 SiO_2, mol%, hot pressed) when removed from the cage wires. The long impressions made by the cage wires are apparent.

ORIGINAL PAGE IS
OF POOR QUALITY

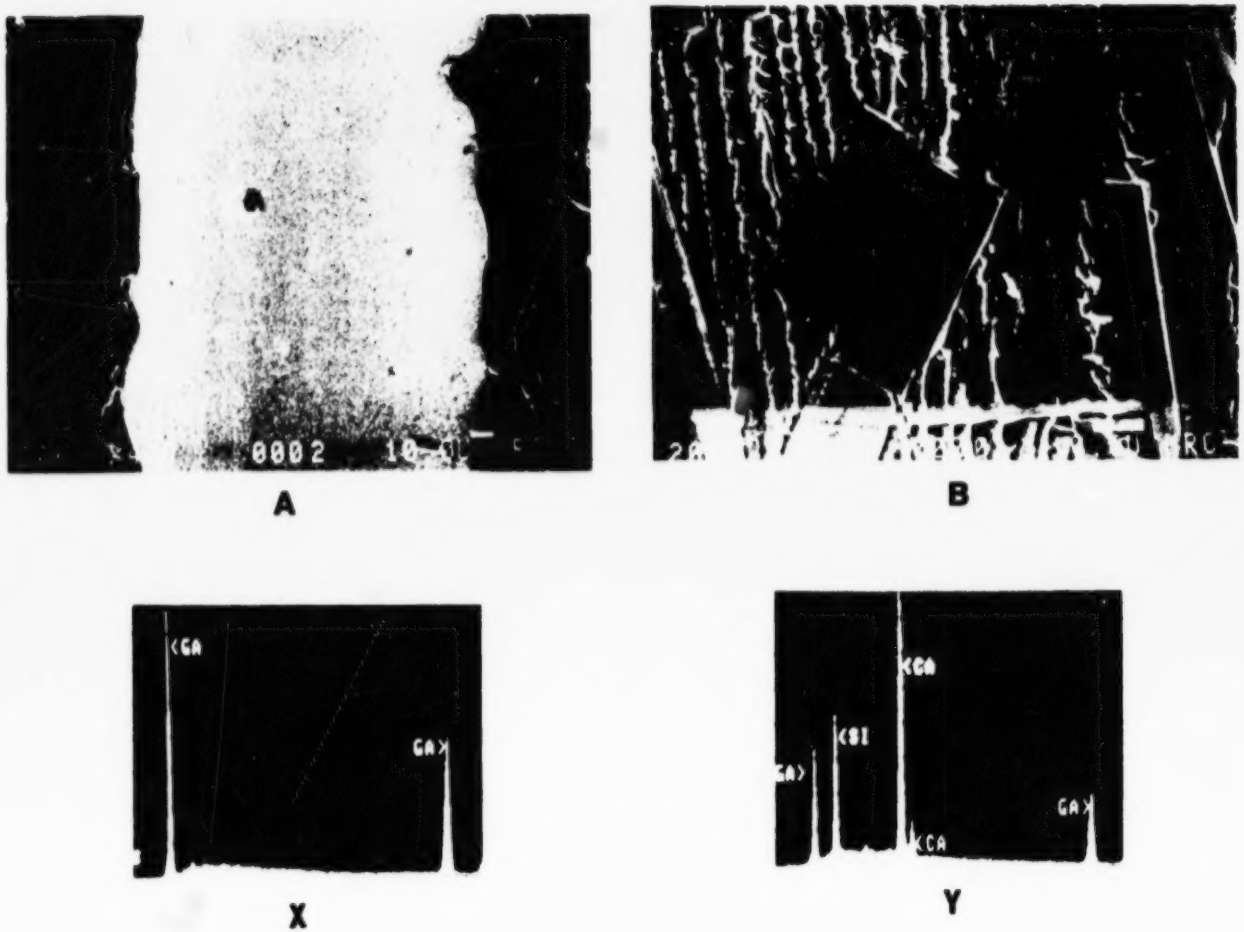

Figure 16. External surface of flight sample 2 (35.7 CaO-39.3 Ga_2O_3-25 SiO_2, mol%, hot pressed) in the vicinity of the vertical platinum wire shown imbedded in the sample in Fig. 11. The wide light band in A is the platinum wire imbedded in the sample. Crystals are visible on both sides of the platinum wire. Two crystalline phases, as shown in B, were observed. The plane flat crystals contain Ga only (see X). The rough needle shaped crystals contain Ca, Ga, and Si (see Y).

ORIGINAL PAGE IS
OF POOR QUALITY

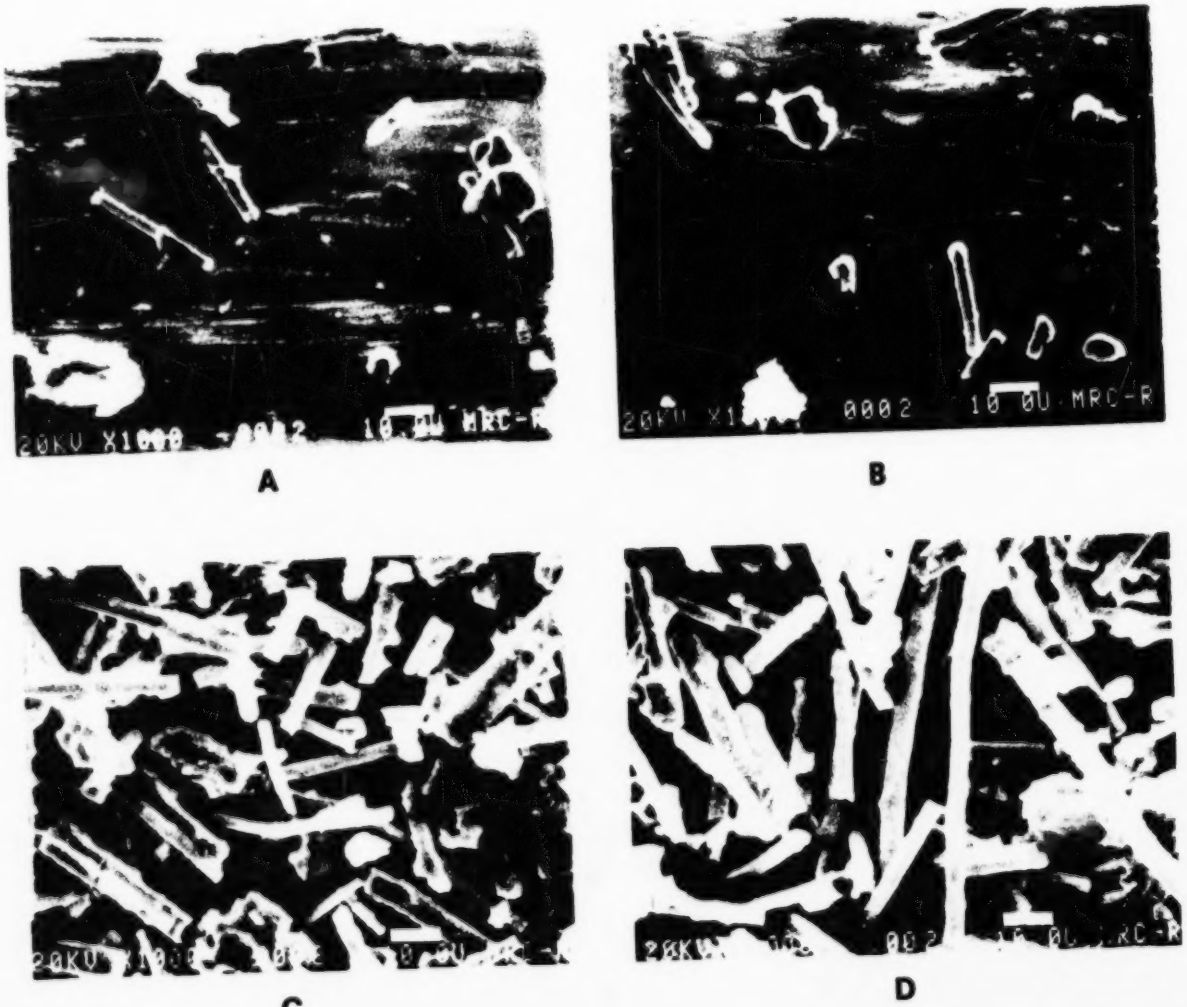

Figure 17. SEM of the external surface of the vertical platinum wire imbedded in the flight sample 2 (see Fig. 11). The platinum wire contains numerous rod shaped fibers on its external surface (A and B). EDAX in (X) shows these fibers contain Al and Si. C and D show fibers of similar shape taken from the furnace insulation and they also contain Al and Si (see Y).

ORIGINAL PAGE IS
OF POOR QUALITY

ORIGINAL PAGE IS
OF POOR QUALITY

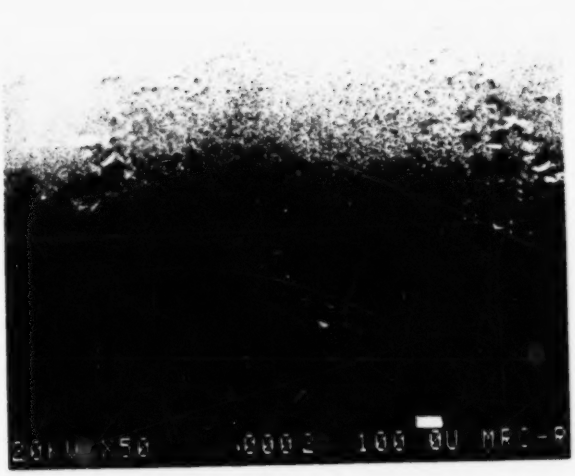

A

B

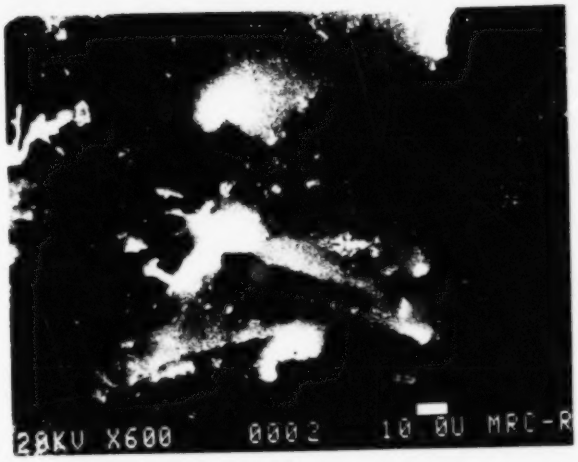

C

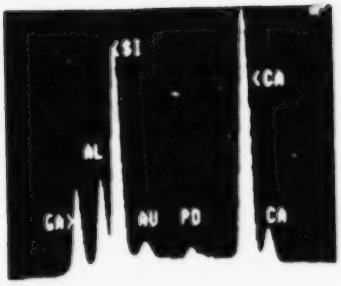

D

Figure 18. Crystallization found on the external surface of flight sample 2 (35.7 CaO-39.3 Ga_2O_3-25 SiO_2, mol%, hot pressed) from surface #1 in Fig. 11. Surface crystallization is seen to initiate from the dark spot at the center of A, which is due to contamination. Enlarged views (B and C) of the dark spot in A show that it contains rod-shaped particles like those shown in Fig. 17. EDAX (D) shows that these particles contain Al and Si. The Ca and Ga in D come from the surrounding matrix.

particles found on the surface of sample 2 are believed to originate from the refractory insulation used in the SAAL. In addition, K, S, and Cl were detected as contamination on the external surface of sample 2, see Fig. 19.

The relative composition at numerous locations on the external surface of sample 2 was determined by EDAX. The average relative composition, based on 15-20 different locations of ≈1600 to 2500 μm^2 in area, on each surface is given in Table X. These results show that the external surface of sample 2 is fairly inhomogeneous. Surface 1 is more inhomogeneous than surface 2, which is consistent with fact that surface 1 was more heavily crystallized than surface 2.

The platinum-rhodium wires imbedded in the sample were removed, and the sample was broken so that its interior could be examined. The interior (bulk) surface of four different fractured pieces of sample 2 was analyzed as shown in Fig. 20, the crystallized region extended (≈1 mm) into the sample only at those points which touched the platinum wires. The crystals at other locations were essentially confined to the external surface. The crystallized region extending into the interior also contained the same two types of crystals found on the external surface. The relative composition determined (by EDAX) at 10-12 different locations in the glassy interior are compared in Fig. 21 with that of the external surface, see Table XI also. The interior (bulk) is considerably more homogeneous than the external surface. The general appearance of the interior of sample 2 is shown in Fig. 22. The 100 to 300 μm silica particles or silica-rich regions initially present in the precursor (Figs. 8 and 9) were not found either on the external surface or in the interior of sample 2. As shown in Fig. 22, a few bubbles (30 to 40, diameter <0.17 mm), were found inside sample 2. The overall results for the external surface and interior of sample 2 are summarized in Figs. 23 and 24, respectively.

ORIGINAL PAGE IS
OF POOR QUALITY

A

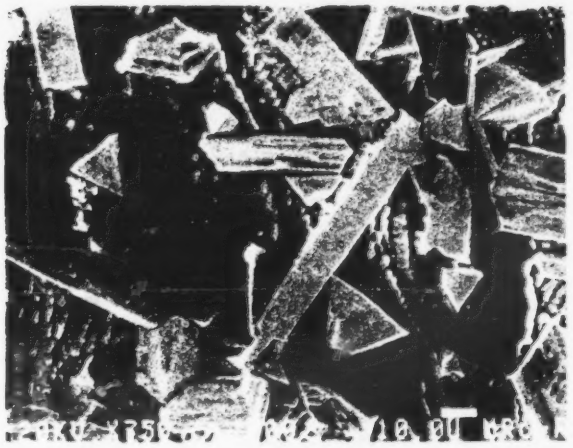

B

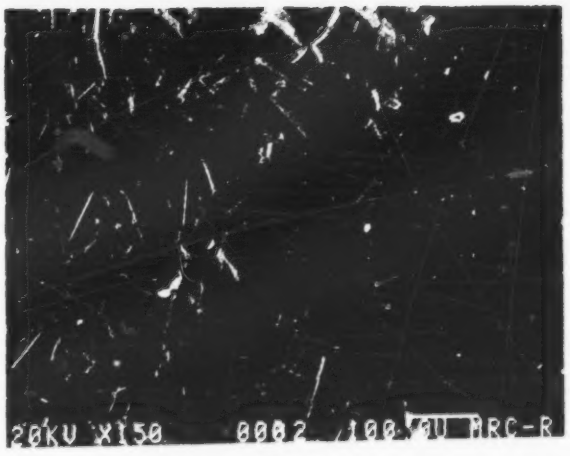

C

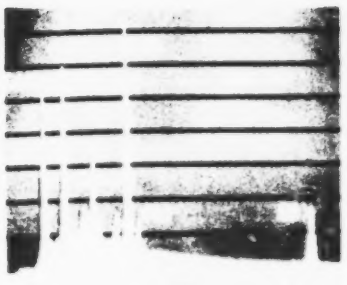

D

Figure 19. Microstructure of the external surface of flight sample 2 (35.7 CaO-39.3 Ga_2O_3-25 SiO_2, mol%, hot pressed) showing crystal concentration at different distances from the vertical platinum wire imbedded in the sample in Fig. 11. A is adjacent to the platinum wire, while B and C are ~0.5 and 1 mm away from the platinum wire, respectively, in the direction of surface 1. Small white spots in B and C are impurities containing K, S, and Cl (see D).

TABLE X. Relative wt% composition (EDAX) of the external surface of sample #2 (calcia-gallia-silica, hot pressed), MEA/A-2 experiment. Typical area analyzed =1600-2500 square micrometers.

Oxides	Surface 1 (in contact with cage)			Surface 2 (not in contact with cage)			Wt% Composition of Precursor
	Max*	Min*	Ave*	Max	Min	Ave	
SiO_2	27.1%	14.9%	21.7%	24.7%	16.4%	21.3%	13.8
CaO	19.7	12.8	17.2	20.2	18.6	19.6	18.4
Ga_2O_3	72.8	54.7	61.2	63.7	56.7	59.1	67.8

*Maximum, minimum, and average wt% of 10-20 different locations.

ORIGINAL PAGE IS
OF POOR QUALITY

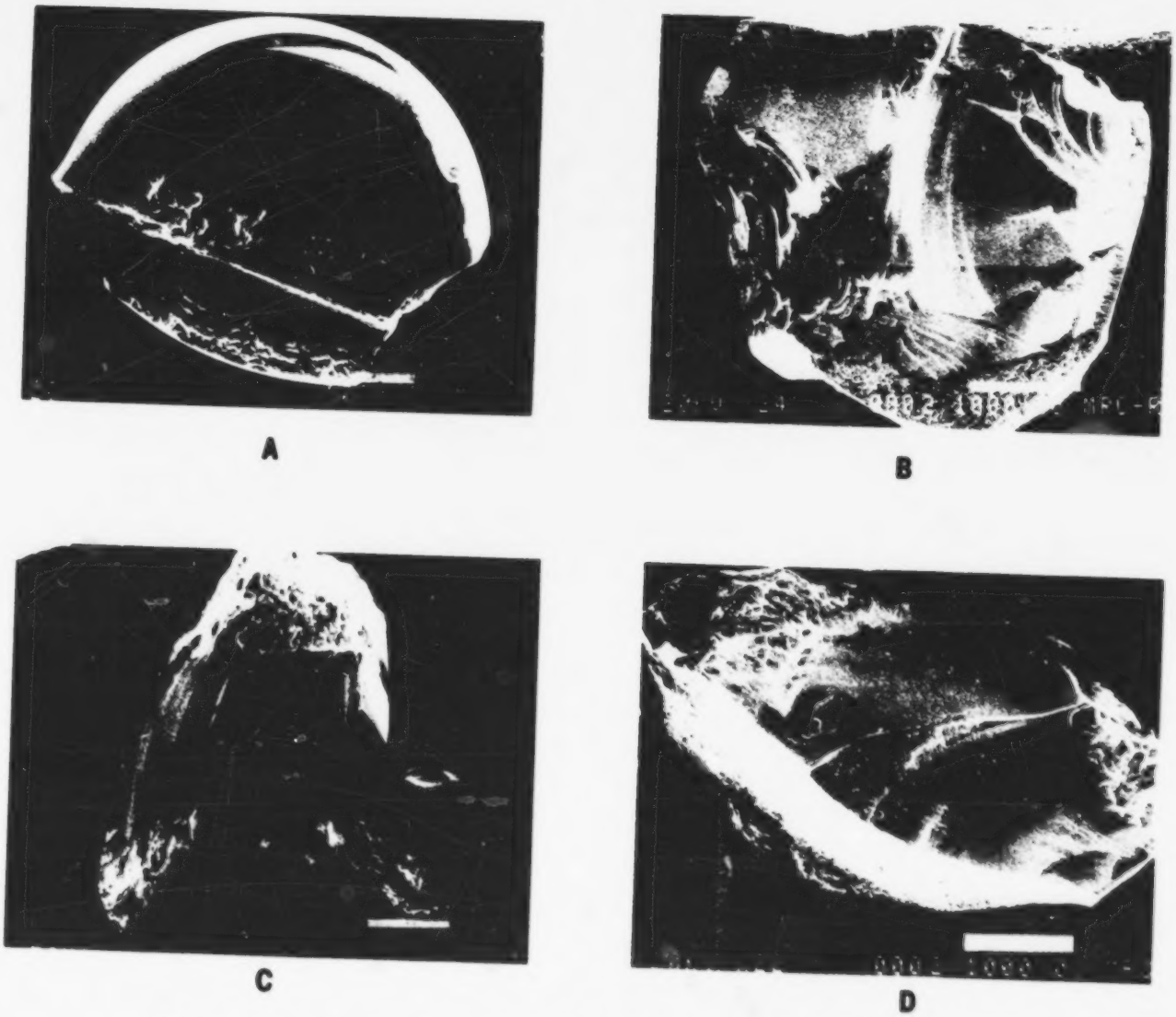

Figure 20. Pieces of flight sample 2 (35.7 CaO-39.3 Ga_2O_3-25 SiO_2, mol%, hot pressed) showing the interior fracture surface examined by SEM. In A and C the crystalline region extended into the bulk ∿1 mm from the imbedded platinum wire. The remaining portion of the bulk is glassy as shown in B and D. This sample is estimated to be 70 to 80% glass. A few small gas bubbles are visible in the center part of C and close to the bottom left side of the piece in D. Fracture surfaces were etched in 2% HNO_3 + HCl solution for 15 seconds at 25°C.

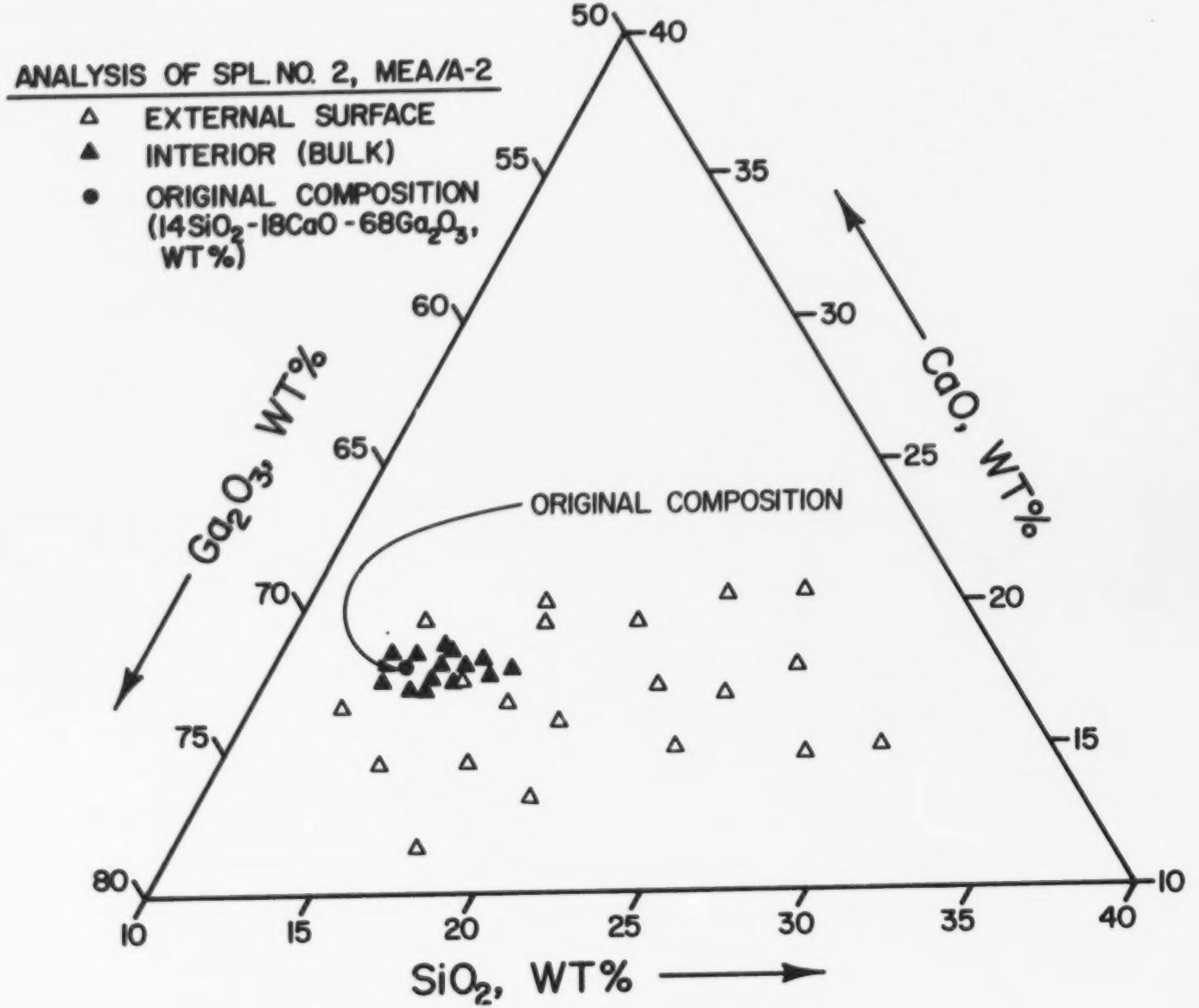

Figure 21. Composition of the external surface and the interior of flight sample 2 (35.7 CaO-39.3 Ga_2O_3-25 SiO_2, mol%, hot pressed) as determined by EDAX.

TABLE XI. Relative wt% composition (EDAX) in the interior of sample #2, MEA/A-2 experiment. Average area analyzed ≈1600-2500 square micrometers.

Oxides	Interior Surface			Wt% Composition of Precursor
	Max*	Min*	Ave*	
SiO_2	18.6%	14.4%	16.6%	13.8
CaO	18.1	17.2	17.7	18.4
Ga_2O_3	68.2	63.5	65.7	67.8

*Maximum, minimum, and average wt% of 10-20 different locations.

ORIGINAL PAGE IS
OF POOR QUALITY

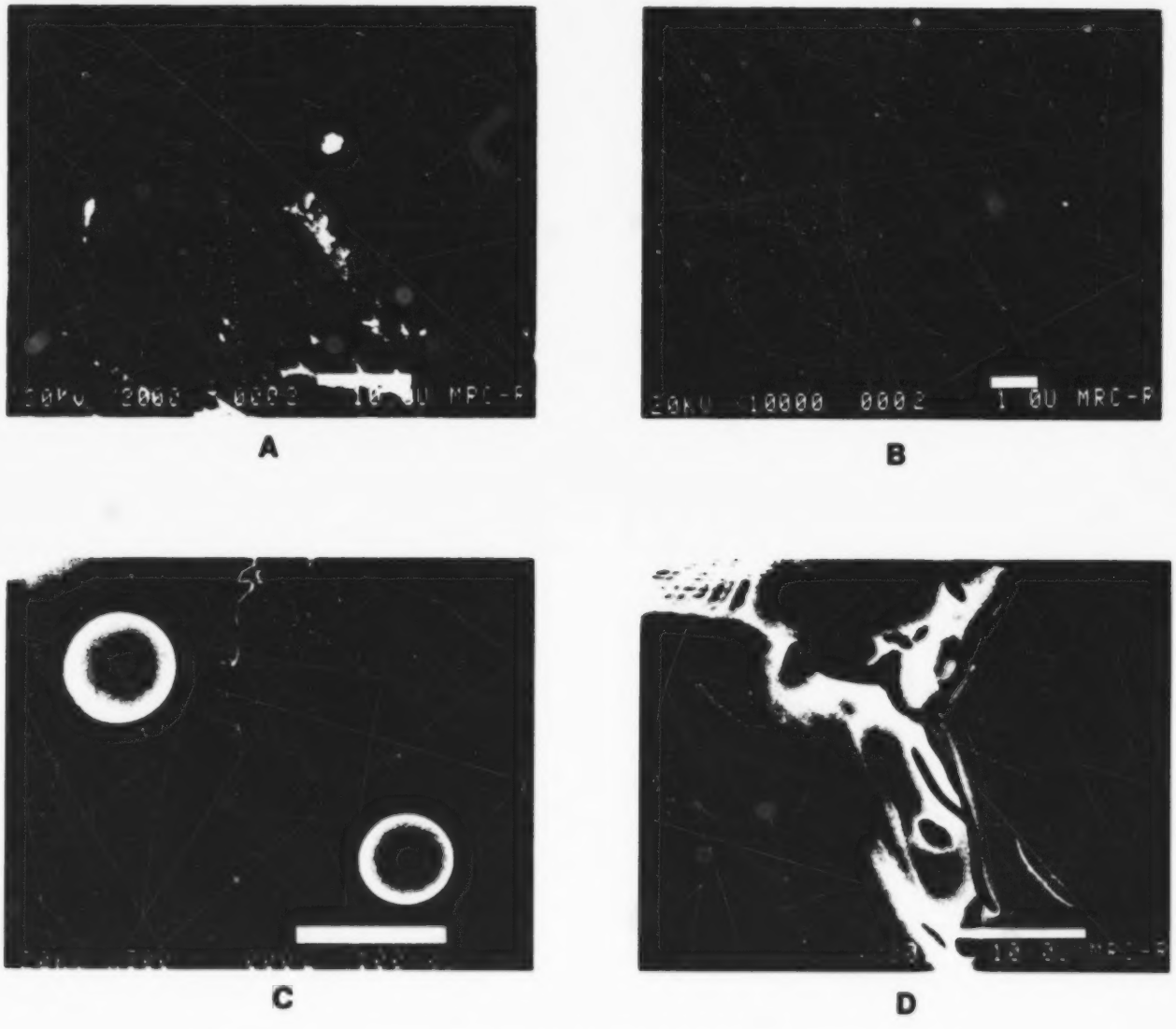

Figure 22. General appearance in the interior of sample 2 (35.7 CaO-39.3 Ga_2O_3-25 SiO_2, mol%, hot pressed). A: glass-crystal interface, B: appearance of glassy region, C: gas bubbles, and D: irregular shaped channels, the source of which are unknown. Surfaces were etched in 2% HNO_3 + HCl solution for 15 seconds at 25°C.

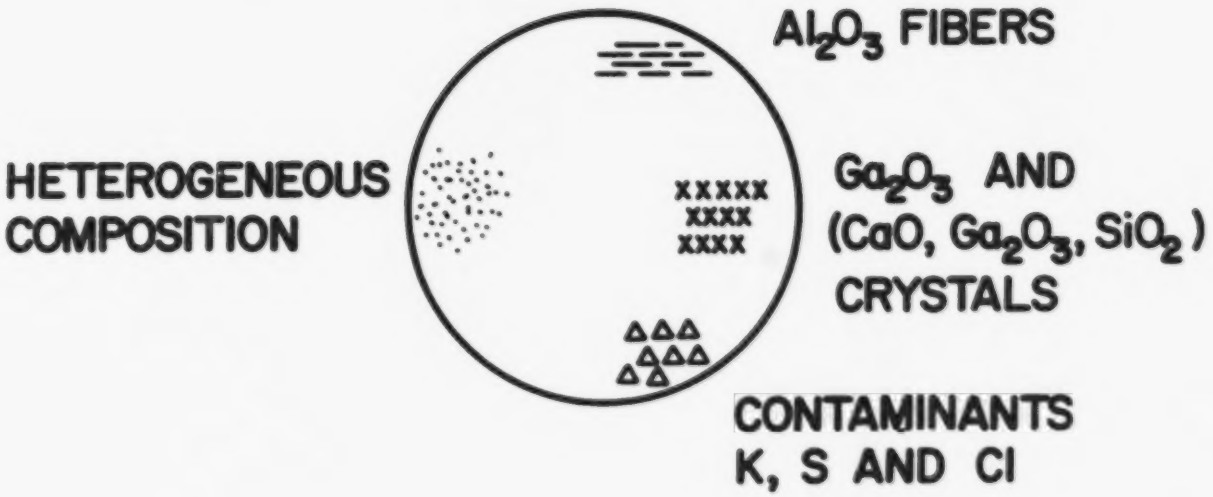

Figure 23. Summary of analysis for the external surface of sample 2 (35.7 CaO-39.3 Ga_2O_3-25 SiO_2, mol%, hot pressed).

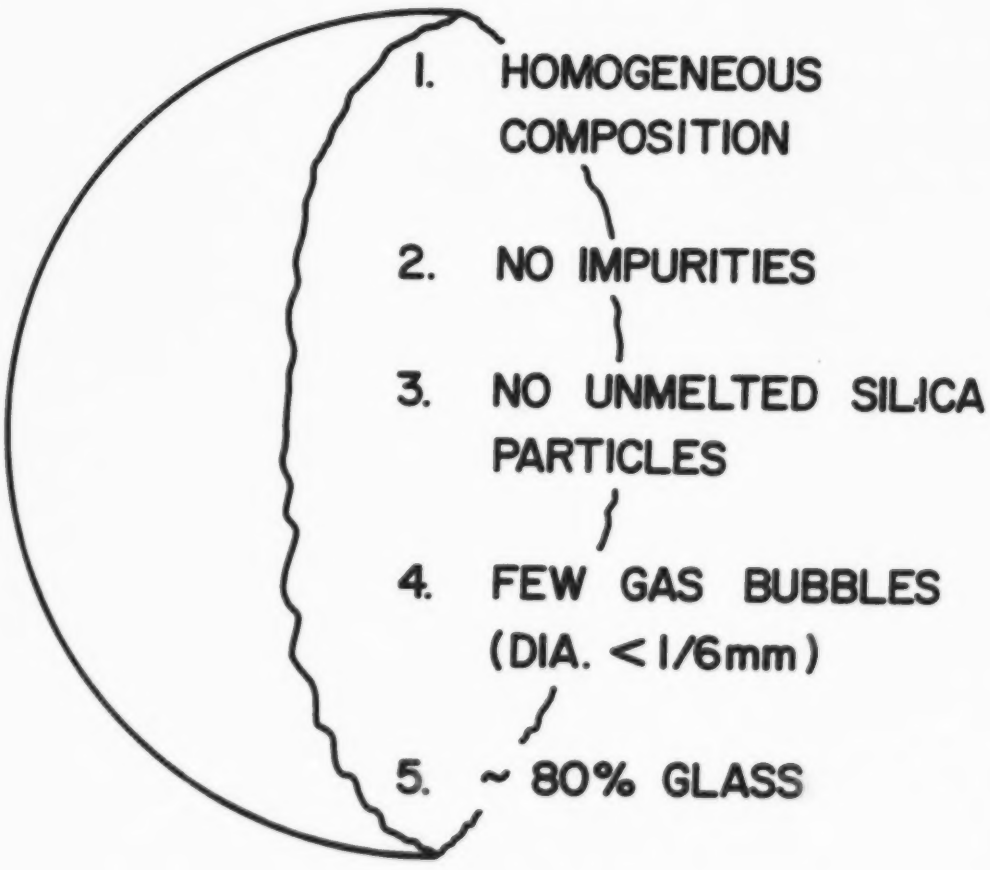

Figure 24. Summary of analysis for the interior of sample 2 (35.7 CaO-39.3 Ga_2O_3-25 SiO_2, mol%, hot pressed).

The examination of flight sample 2 indicates that it contains 70 to 80% glass and the remainder is crystalline. It is believed that this sample would have been totally glassy if it did not collide with the cage since only that portion contacting the platinum wires crystallized. The average cooling rate between 1450 and 1000°C, as calculated from the time-temperature data from the flight recorder on MEA/A-2, was 4.2°C/s. This is lower than the cooling rate of 11.3°C/s, which was required to form glass on earth for a sample of identical size, by a factor of 2.7. This indicates that the glass formation tendency of this calcia-gallia-silica composition is improved by a factor of between 2 and 3 when melted in a containerless manner in space. Based on the cooling rate data measured on earth, a TTT diagram for this glass with a sample diameter 6.5 mm (identical to sample 2, MEA/A-2) has been estimated and is drawn in Fig. 25. Superimposed on the TTT diagram is the actual cooling curve of flight sample 2 which is seen to intersect the crystallization region inside the TTT diagram. This indicates that a sample cooled on earth at a rate equal to that used in the flight experiment would be totally crystalline. The fact that the sample returned partially glassy clearly demonstrates that containerless melting increases the glass formation tendency of this calcia-gallia-silica composition. The analysis of this sample is summarized in Table XII.

Sample 3 (Soda-Lime-Silica Glass Shell). As mentioned earlier, this glass macro shell was used primarily to assess the feasibility of removing irregularities from its inner surface and reshaping it in micro-g into a highly spherical shell of uniform wall thickness. Radiographic analysis of the post flight sample confirmed that it was no longer a shell, but an ell p-soidal (egg-shaped) piece of solid glass. The largest to smallest diameter differed by ~0.521 mm (diameter, max = 5.334, min = 4.813 mm). Fig. 26 compares the radiographs of the pre- and post-flight samples. The large bubble

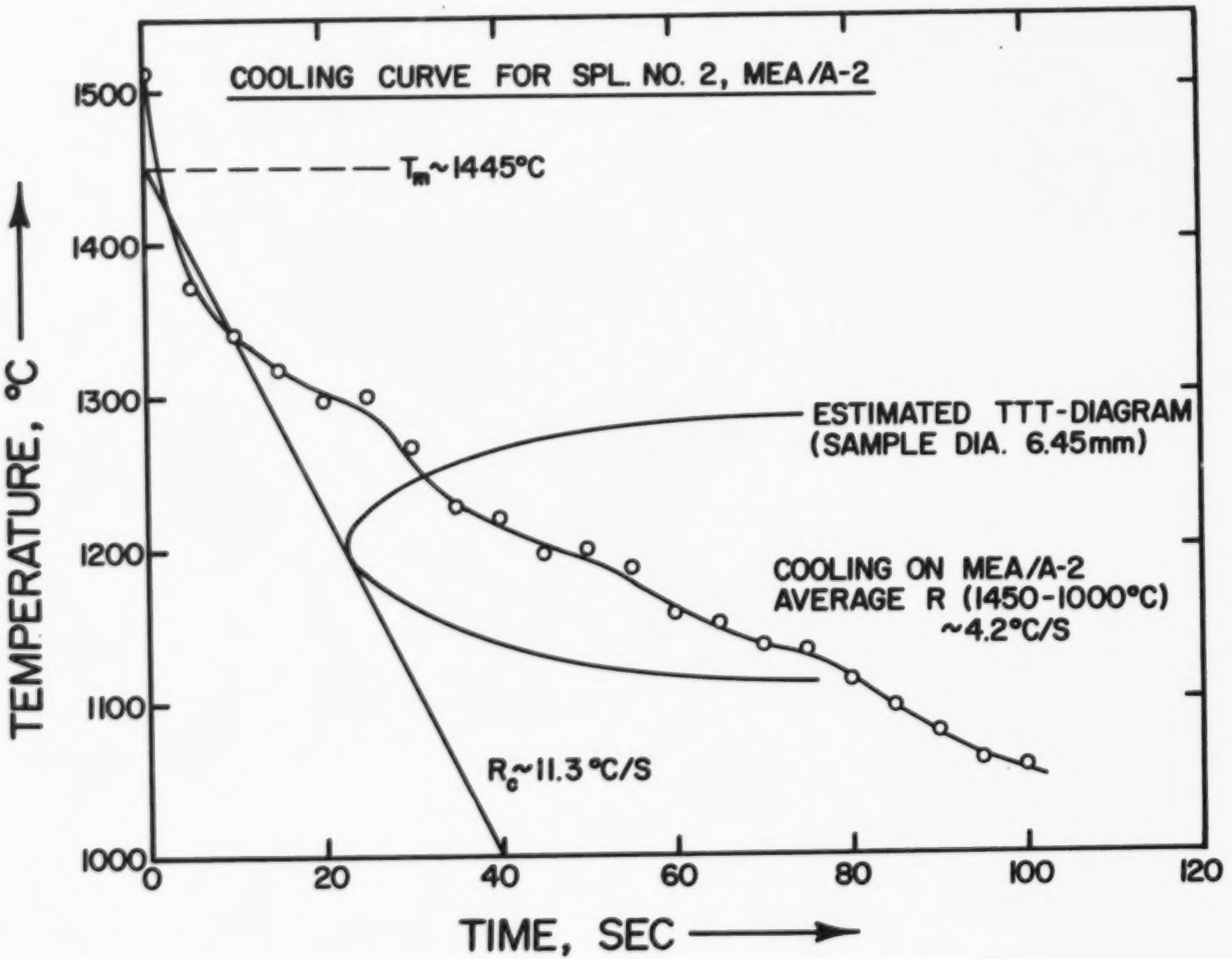

Figure 25. The estimated TTT diagram for the 35.7 CaO-39.3 Ga_2O_3-25 SiO_2, mol%, composition for sample diameter ~6.5 mm and the cooling rate measured for sample 2 in MEA/A-2.

TABLE XII. Results for the hot pressed calcia-gallia-silica sample (#2) processed on MEA/A-2 experiment.

1. The sample escaped the acoustic energy well and stuck to the cage wires while levitated in the SAAL in space. Escape was clearly associated with the opening of the SAAL cooling shroud gate.

2. 70 to 80% of the sample was glassy. Partial crystallization (~20%) was observed where the melt touched the platinum wires of the cage. Examination by SEM and EDAX showed that the crystalline phases were Ga_2O_3 and $Ca_2Ga_2SiO_7$.

3. Comparison of the critical cooling rate for glass formation of this glass on earth with the cooling rate used in the flight experiment, showed a 2 to 3 times enhancement of glass formation for this composition melted in space.

4. The large silica particles (100-300 μm) initially present in the precursor were undetectable in the flight sample.

5. The interior of the sample was more chemically homogeneous than the external surface.

6. Impurities such as S, K, Cl, and the furnace insulation (aluminum silicate) were found on the external surface of this sample.

7. A few spherical gas bubbles < 0.17 mm in diameter were present in the interior of this sample.

8. No significant difference in properties was found for the glass made in space or on earth.

9. Hot pressing is a feasible means of preparing precursor samples.

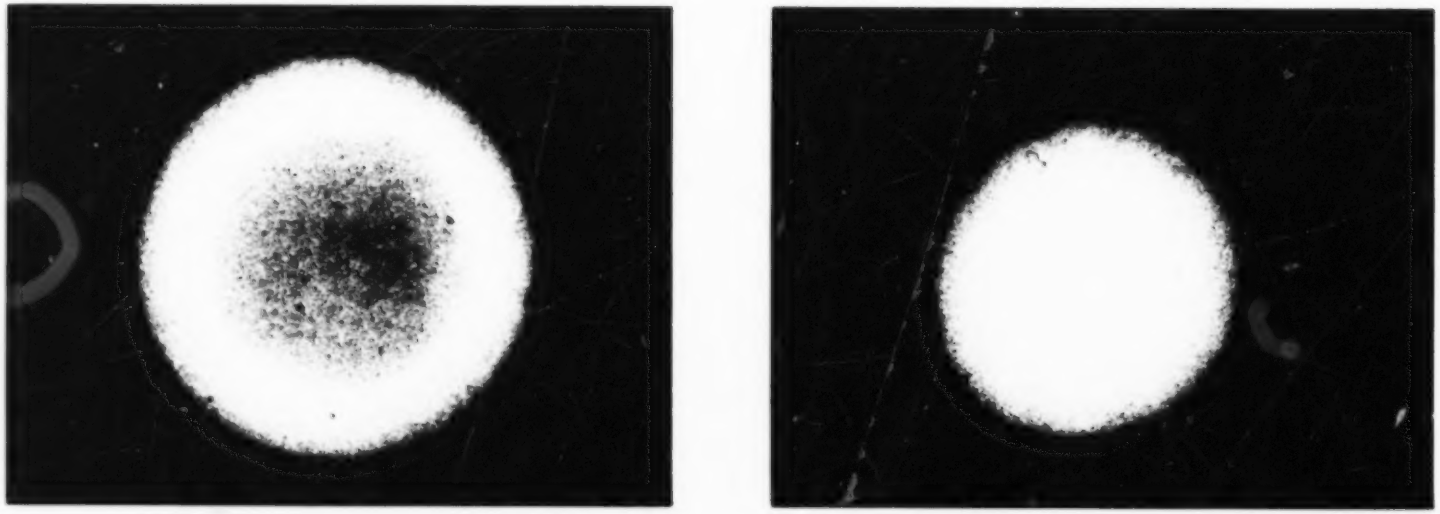

ORIGINAL PAGE IS
OF POOR QUALITY

Figure 26. Radiographs of the (A) pre- and (B) post-flight sample 3 (soda-lime-silica glass shell). The bubble initially present in the center of the pre-flight sample is clearly visible in A. No bubble is visible in the post-flight sample (B).

and the inner surface-irregularities present inside the pre-flight sample are clearly visible, but no bubble is visible in the post-flight sample. Measurements show that surface finish of the post-flight sample is very smooth, equivalent to a fire polish surface. The largest peak to valley roughness on the surface is ≈135 A°, with a maximum root mean square (RMS) value ≈21 A°. Compositional analysis of the external surface indicates that unlike sample 2, this sample was not contaminated by any foreign material. The overall analysis results of this sample are summarized in Table XIII.

The reason why the bubble escaped from sample 3 and how it deformed to an ellipsoidal shape is not clear at this point. One possible explanation for the escape of the bubble is the existence of a temperature gradient, which might establish a surface tension gradient in the sample. Marangoni flow could cause the bubble to move to the region of lower surface energy and to eventually escape from the sample. The present SAAL is not equipped with a sufficient number of thermocouples to assess the magnitude of any temperature gradients. However, the existence of temperature gradients is not inconceivable in the present furnace.

The effect of spinning (while molten and levitated) on the shape of the sample was examined theoretically. Calculations show that a rotational speed of ≈1220 rpm would be required to produce the shape and dimensions identical to flight sample 3. There is no definite evidence showing that the sample was spinning while molten, but this speed is considered unrealistically high. Another possibility is that the sample was deformed by acoustic forces since recent calculations[20] indicate that these forces increase during cooling and may not be negligible as previously assumed.

TABLE XIII. Results for the soda-lime-silica glass shell (#3) processed on the MEA/A-2 experiment.

1. The bubble initially present escaped from the sample while it was levitated at 1250°C in the SAAL.
2. The returned sample was an ellipsoidal piece of solid glass whose maximum and minimum diameter was 5.334 and 4.813 mm, respectively.
3. The external surface of the sample was extremely smooth, having a root mean square peak to valley roughness of only 21Å.
4. No contamination was found on the external surface of this sample.

E. Comparison of Properties for the Glasses Melted in MEA/A-2 (Sample #2) and on Earth

Due to the small sample size and partial devitrification of flight sample 2, only a few properties could be measured. The refractive index, dispersion, and Abbe number for this glass were measured using the Becke line technique. These values are compared with those of a glass of identical composition melted on earth in Table XIV. The properties are slightly different for the two glasses. The crystallization behavior of the space- and earth melted glasses were also studied by differential thermal analysis (DTA) at a heating rate of 10°C/min. A comparison of the DTA curves in Fig. 27 shows that the crystallization for the space and earth melted glasses is essentially identical. The appearance of a large exothermic peak with a small shoulder on the low temperature side in the DTA curve shows that two compounds crystallize from this glass. They have been identified by XRD analysis as β-Ga_2O_3 and $Ca_2Ga_2SiO_7$ ($2CaO \cdot Ga_2O_3 \cdot SiO_2$). The same two phases were also observed when the crystallized region of the space melted sample (#2) was examined by SEM (Fig. 16). The larger peak at ≈887°C in Fig. 27 has been found to correspond to the crystallization of $Ca_2Ga_2SiO_7$. This has been determined by examining the crystallization behavior of a glass whose composition is $2CaO \cdot Ga_2O_3 \cdot SiO_2$. The smaller peak (855°C) in Fig. 27 is attributed to the crystallization of β-Ga_2O_3.

The infrared transmission of the space and earth-melted glasses and their devitrified counterparts were also measured and are compared in Figs. 28 and 29. No significant difference in the IR transmission of these two glasses is observed.

TABLE XIV. Refractive index, dispersion, and Abbe number for the 35.7 CaO-39.3 Ga_2O_3-25 SiO_2, mol% glass melted in space and on earth.

	Space Sample MEA/A-2, Spl. #2	Earth Sample
Refractive Index (± 0.0010)	1.7287	1.7121
Dispersion	0.0279	0.0175
Abbe Number (± 3.5)	26.1	40.5

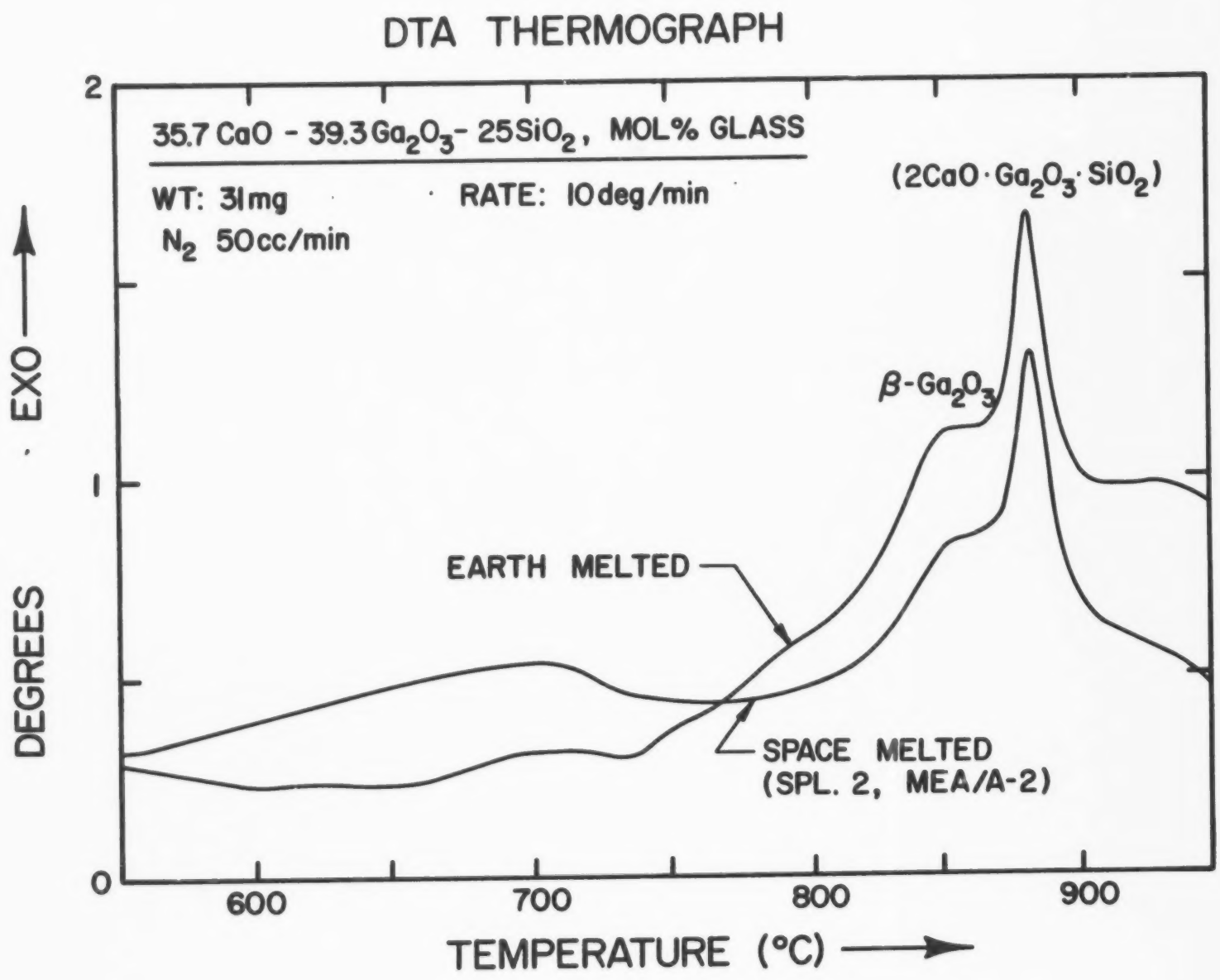

Figure 27. DTA thermogram for the 35.7 CaO-39.3 Ga_2O_3-25 SiO_2, mol%, glasses melted in space (MEA/A-2) and on earth.

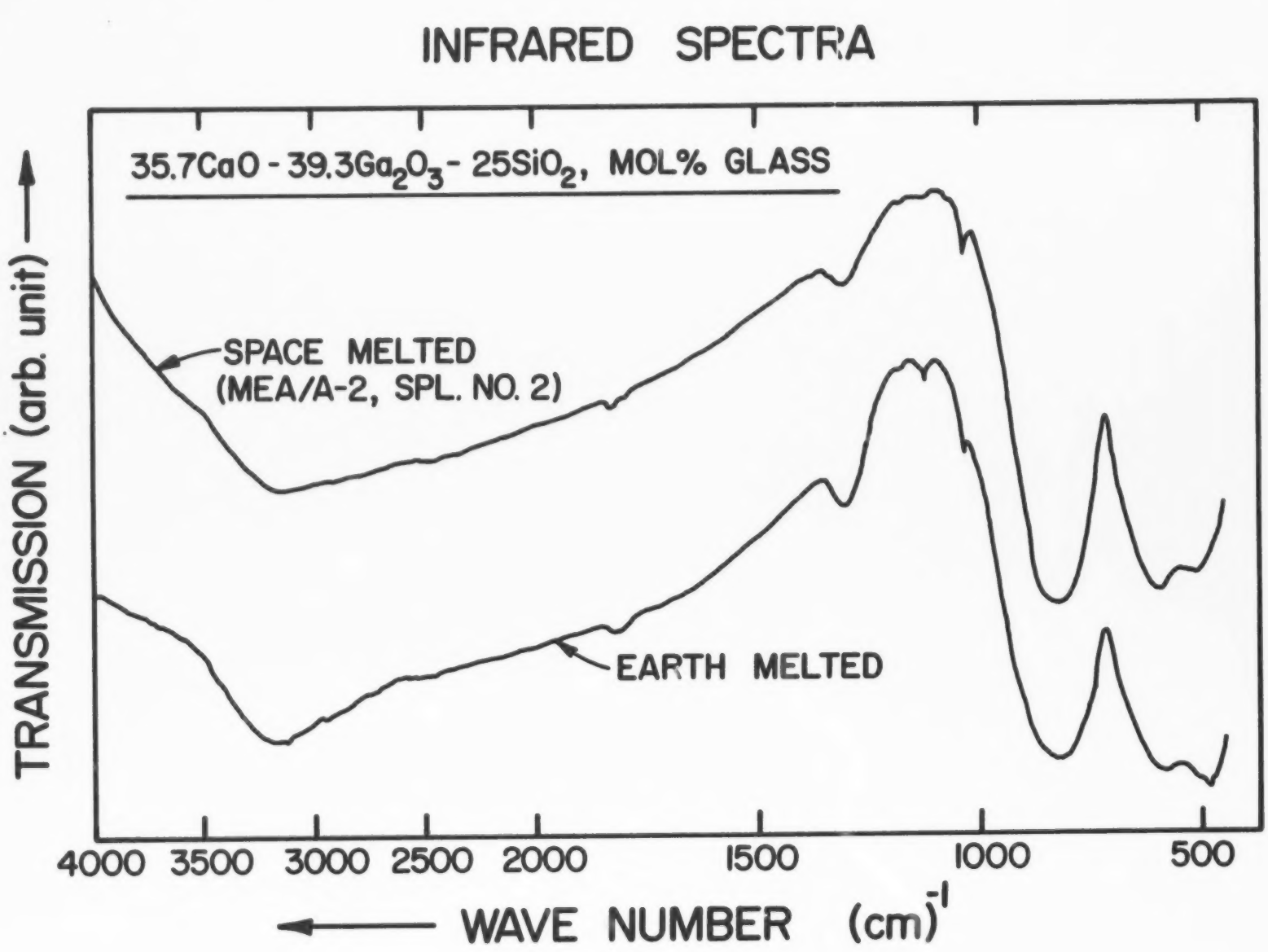

Figure 28. IR transmission for the 35.7 CaO-39.3 Ga_2O_3-25 SiO_2, mol%, glasses melted in space (MEA/A-2) and on earth.

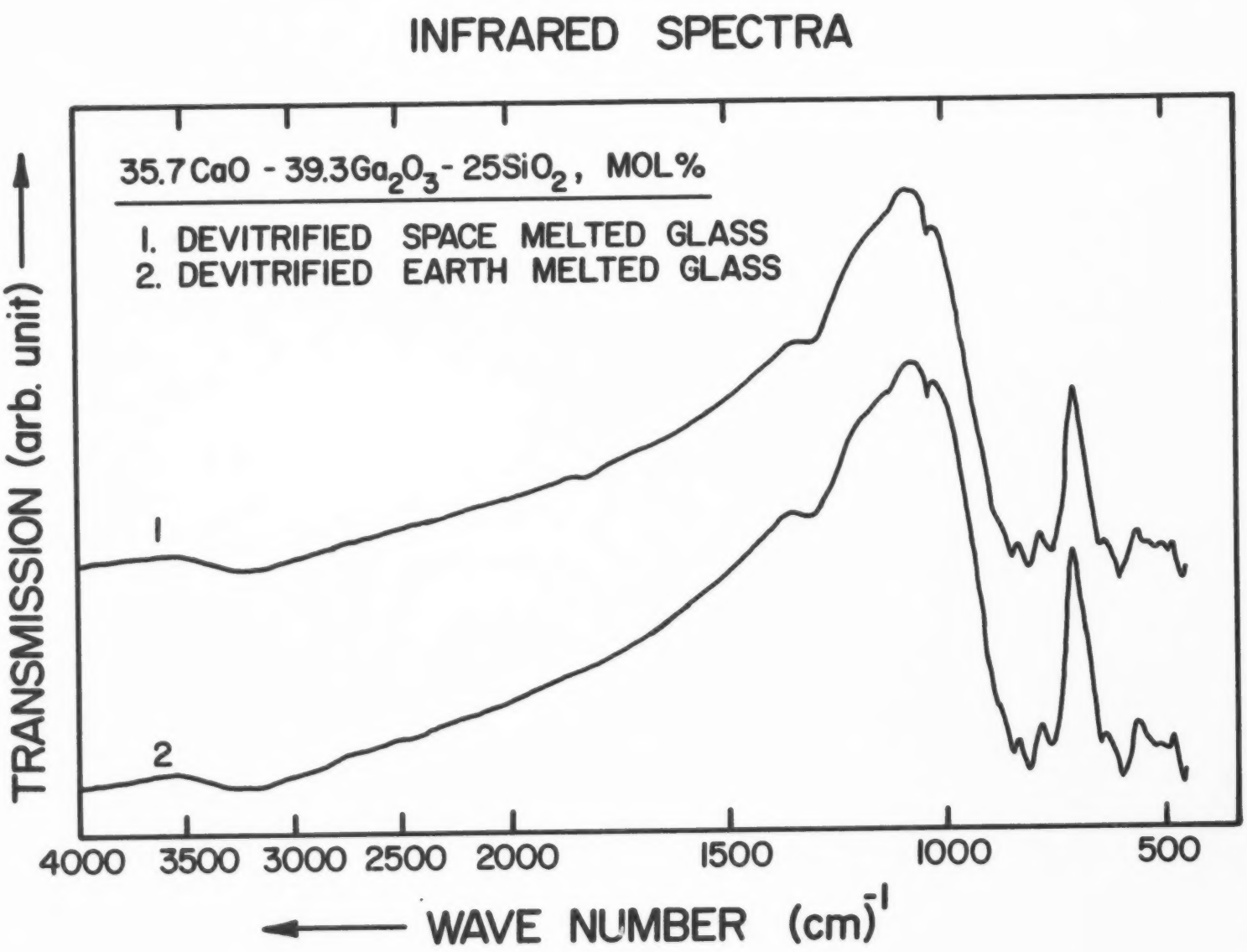

Figure 29. IR transmission for the devitrified 35.7 CaO-39.3 Ga_2O_3-25 SiO_2, mol%, glasses melted in space (MEA/A-2) and on earth.

VI. CONCLUSIONS

The conclusions summarized below for the MEA/A-2 flight experiment are listed in the order of the objectives for this experiment.

A. Operational Assessment of SAAL

1. The operation of the single axis acoustic levitator/furnace in space for high temperature liquid samples was generally satisfactory. For the first time, liquid samples were successfully levitated in space at high temperatures (1250 to 1500°C) for a considerable period of time (6 to 10 min). The mechanism for sample insertion operated as intended for the first three samples, but the samples were not recaptured (clamped) by the cage and alumina tube as intended at the completion of the cooling phase. The temperature-time profile of the furnace was close to that programmed for samples 1, 2, and 3, but the furnace did not operate for the remaining five samples (4 through 8).
2. An excellent photographic (movie) record of the sample processing sequences in microgravity was obtained. The film gives a good optical view of the samples and their movements at temperatures above 800°C, but the resolution/clarity is not adequate for detailed observation of the sample. Bubbles or other objects less than≈1 mm are not easily observed.
3. The following recommendations are made to improve the operational performance of the SAAL.
   a) Contamination of the samples from all sources but especially from the furnace insulations, needs to be eliminated when the molten samples are levitated in space.
   b) The samples should be released in a smoother and gentler fashion so as to eliminate the temporary oscillation and positional instability that now occurs.

c) The furnace should hold a more constant temperature (± 10°C max) when being controlled at a fixed temperature.

d) Improvements in the stability of the sample in the acoustic well are highly desirable and events (opening and closing of gates) which upset the sample stability should be avoided. The cooling shroud gate should not be used in the future for liquid samples unless there is no concern about the sample contacting the platinum cage wires.

e) It is desirable to have the capability to reduce the acoustic forces (sound field intensity) used to levitate liquid samples so as to avoid or minimize the distortion of such samples during cooling.

f) Provision to obtain slower, but controlled cooling rates by partial reduction of the electrical power to the furnace is desirable.

g) Additional thermocouples should be installed in the vicinity of the sample to better assess the sample temperature and the temperature uniformity in that region of the furnace occupied by the sample. Sample temperature measurement with an optical pyrometry (or other non-contact method) would be highly useful.

h) Improved resolution and higher magnification for photographing the sample during processing in the SAAL is desirable.

B. Enhanced Glass Formation

Two glass forming samples (calcia-gallia-silica and soda-lime-silica) were successfully melted and cooled to glass while levitated in space. The calcia-gallia-silica composition requires a cooling rate ≈11°C/s to form glass

on earth for the sample size used in the space experiment. This cooling rate is 2 to 3 times higher than the cooling rate (≈4°C/s) for the MEA/A-2 experiment which yielded a glass for this composition. Clearly, the glass formation tendency for this calcia-gallia-silica composition is increased by 2 to 3 times when melted in space without a container.

C. Melt Homogenization and Precursor Preparation Technique

A usable and homogeneous glass was obtained for the hot pressed calcia-gallia-silica composition for the melting time and temperature used in the flight experiment. This hot pressed sample was prepared from crystalline powders containing randomly distributed heterogeneities up to 300 μm in size. Chemical homogenization of this melt is reasonably fast in space in the absence of gravity-driven convection. Hot-pressing appears to be a feasible way to prepare chemically ultra-pure samples for materials processing in space.

D. Comparison of Properties

The comparison of selected properties for the space and earth melted calcia-gallia-silica glass shows that the refractive index, dispersion and Abbe number are slightly different, but there is no detectable difference in their infrared transmission or crystallization behavior. For this particular glass composition, melting in space produced no important difference in properties.

E. Shaping

The soda-lime-silica glass shell was used primarily for the purpose of demonstrating the feasibility of reshaping a glass shell in microgravity. Since the bubble escaped when the sample was remelted in space and the sample returned as a solid, egg-shaped piece of colorless glass, the feasibility of shaping a glass shell in microgravity has not been demonstrated. The reshaping of glass shells in space is still considered feasible and possible once

the mechanism responsible for the bubble motion and that causing the deformation of the sample have been identified and are controllable.

F. Other

The performance and suitability of the samples used in the flight experiment was satisfactory. No mechanical damage (due to vibration of the shuttle), chemical attack, or change in weight of the samples was observed. The procedure followed in preparing, handling, and storing the samples is satisfactory.

Based on the performance of the SAAL and the results obtained for the glass melting experiments, it is believed that a considerable advancement has been achieved in the science and technology of materials processing in space. Nevertheless, the basic scientific objectives regarding enhanced glass formation, melt homogenization and mixing, bubble behavior, and reshaping simple shapes in space are still to be completely fulfilled. The results of this experiment which demonstrate the enhancement of glass formation in space are highly encouraging and need to be verified for other potentially useful compositions.

Our ground based research program remained highly active and valuable scientific data for the glass formation, nucleation and crystallization, structure and property relationship of several interesting glass systems were obtained. Since 1983, this research has been reported in 14 technical papers, 12 of which have been published in the open literature and 2 of which are in press (see Appendix A).

VII. ACKNOWLEDGEMENTS

The authors would like to acknowledge the containerless processing of glass forming melts is sponsored by NASA Headquarters Microgravity Science and Applications Division. This makes possible the multidisciplinary effort to heat, melt, and quench spherical samples of different glass forming compositions while they are levitated in a single-axis acoustic levitator furnace.

Also, the authors would like to thank the Application Payload Projects Office of the Spacelab Payload Project Office, Marshall Space Flight Center, AL, for their invaluable assistance in programming and integrating of this experiment into the space transportation system.

The authors are deeply indebted to Dr. N. J. Kreidl, consultant, for many helpful discussions and suggestions. Our special appreciation is extended to Dr. R. S. Subramanian of Clarkson University for providing the sodium-borate sample (#5), to Mr. F. Gac of Los Alamos National Laboratory for supplying the soda-lime-silica hollow glass shell (#3), and to Dr. C. Rey of Intersonics, Inc., for many practical suggestions. The technical assistance of S. Sensarma, I. N. Chakraborty, G. Whichard, H. Rutz, P. Angel, and T. Neidt is also acknowledged.

REFERENCES

1. N. J. Kreidl and G. E. Rindone, J. Non-Cryst. Solids, 38 and 39, 825 (1980).
2. D. R. Uhlmann, Glass Processing in Microgravity Environment in "Materials Processing in the Reduced Gravity Environment of Space", Ed. G. E. Rindone, Elsevier Sci. Publ. Co., N.Y., 1982, p. 269.
3. N. J. Kreidl, D. E. Day, and C. S. Ray, Glastech. Ber., 56K, 151 (1983).
4. C. S. Ray and D. E. Day, National SAMPE Technical Conference Series, 15, 135 (1983).
5. N. J. Kreidl, J. Non-Cryst. Solids, 80, 587 (1986).
6. D. E. Day and C. S. Ray, Research on Containerless Melts in Space, in "Opportunities for Research in a Low Gravity Environment", American Institute for Aeronautics and Astronautics, 1986 (in press).
7. C. Barta, J. Trnka, A. Triska, and M. Frumar, Adv. in Space Res., 1, 121 (1981).
8. G. H. Frischat, K. Herr, H. J. Basklage-Hilgefort, and W. Beier, Glastech. Ber., 53, 1 (1980).
9. W. Beir, M. Braedt, and G. H. Frischat, Phys. and Chem. Glasses, 24, 1 (1983).
10. R. Subramanian, AI. Ch. E. Journal, 27, 646 (1981).
11. P. Annamalai, N. Shankar, R. Cole, and R. Subramanian, Applied Scientific Research, 38, 179 (1982).
12. P. I. K. Onorato, D. R. Uhlmann, and R. W. Hopper, J. Non-Cryst. Solids 41, 189 (1980).
13. D. R. Uhlmann, J. Non-Cryst. Solids 7, 337 (1972); ibid 25, 42 (1977).
14. H. Yinnon and D. R. Uhlmann, J. Non-Cryst. Solids 44, 37 (1981).
15. W. D. Kingery, H. K. Bowen, and D. R. Uhlmann, Introduction to Ceramics, John Wiley and Sons, NY, 1976, p. 347.

16. R. Grange and J. M. Kiefer, Trans. ASM, 29, 85 (1941).

17. R. A. Happe, NASA Technical Memorandum 82433, Space Processing Applications Rocket, Project SPAR VI Final Report, October 1981, Chapter III.

18. R. A. Happe and K. S. Kim, NASA Technical Memorandum 82578, Space Processing Applications Rocket, Project SPAR VIII Final Report, June 1984, Section III.

19. D. E. Day and C. S. Ray, Final Report for MEA/A-1 Experiment 81F01, NASA Contract NAS 8-34758, April 1984, Submitted to George C. Marshall Space Flight Center, Huntsville, Alabama.

20. C. Rey, Intersonics, Inc., personal communication.

APPENDIX A

List of Publications Supported by the Present Contract, NAS 8-34758

1. Crystallization Kinetics of $2Bi_2O_3$-$3GeO_2$ Glass, C. S. Ray and D. E. Day, Proceedings of the 15th North American Thermal Analysis Society Conference, p. 353, 1986.
2. Crystallization of La_2O_3-B_2O_3 Glasses Containing Al_2O_3 or Y_2O_3, C. S. Ray, D. E. Day, and I. N. Chakraborty, Proceedings of the XIV International Congress on Glass, Vol. 1, p. 386, 1986.
3. Crystallization of Baria-Titania-Silica Glasses, C. S. Ray and D. E. Day, J. Non-Cryst. Solids, 81, 173 (1986).
4. Glass Formation, Properties and Structure of Y_2O_3-Al_2O_3-B_2O_3 System, I. N. Chakraborty, H. L. Rutz, and D. E. Day, J. Non-Cryst. Solids, 84, 86 (1986).
5. Dependence of the Critical Cooling Rate for Lithium-Silicate Glass on Nucleating Agents, W. Huang, C. S. Ray, and D. E. Day, J. Non-Cryst. Solids, 86, 204 (1986).
6. Glass Formation and Properties in the System Calcia-Gallia-Germania, P. Angel, C. S. Ray, and D. E. Day, J. Am. Ceram. Soc., 68, 637 (1985).
7. Effect of R^{3+} Ions on the Structure and Properties of Lanthanum-Borate Glasses, I. N. Chakraborty and D. E. Day, J. Am. Ceram. Soc., 68, 641 (1985).
8. Structure Property Relations in Lanthanide-Borate Glasses, I. N. Chakraborty, D. E. Day, J. C. Lapp, and J. E. Shelby, J. Am. Ceram. Soc., 68, 368 (1985).
9. Crystallization of Calcia-Gallia-Silica Glasses, C. S. Ray and D. E. Day, J. Am. Ceram. Soc., 67, 806 (1984).

10. Glass Formation and Properties in the Gallia-Calcia System, G. Whichard and D. E. Day, J. Non-Cryst. Solids, 66, 677 (1984).

11. Description of the Containerless Melting of Glass in Low Gravity, C. S. Ray and D. E. Day, National SAMPE Technical Conference Series (P.O. Box 613, Azusa, CA 91702), 15, 135 (1983).

12. Containerless Glass Processing in Space, N. J. Kreidl, D. E. Day, and C. S. Ray, Glastechn. Ber., 56K, 151 (1983).

13. Research on Containerless Melts in Space, D. E. Day and C. S. Ray, AIAA Journal (in press). Presented in the NSF Workshop, July 10-11, 1985, Washington, DC.

14. Crystallization Kinetics of Lithia-Silica Glasses: Effect of Composition and Nucleating Agent, C. S. Ray, W. Huang, and D. E. Day, J. Am. Ceram. Soc. (in press).